Zoological Journal of the Linnean Society, 2019, **XX**, 1–34. With 11 figures.

The phylogenetic relationships of neosuchian crocodiles and their implications for the convergent evolution of the longirostrine condition

SEBASTIAN S. GROH[1,2,*], PAUL UPCHURCH[1], PAUL M. BARRETT[2] and JULIA J. DAY[3]

[1]*Department of Earth Sciences, University College London, Gower Street, London, WC1E 6BT, UK*
[2]*Department of Earth Sciences, Natural History Museum, Cromwell Road, London, SW7 5BD, UK*
[3]*Department of Genetics, Environment and Evolution, University College London, Gower Street, London, WC1E 6BT, UK*

Received 19 April 2019; revised 28 August 2019; accepted for publication 7 September 2019

Since their origin in the Late Triassic, crocodylomorphs have had a long history of evolutionary change. Numerous studies examined their phylogeny, but none have attempted to unify their morphological characters into a single, combined dataset. Following a comprehensive review of published character sets, we present a new dataset for the crocodylomorph clade Neosuchia consisting of 569 morphological characters for 112 taxa. For the first time in crocodylian phylogenetic studies, quantitative variation was treated as continuous data (82 characters). To provide the best estimate of neosuchian relationships, and to investigate the origins of longirostry, these data were analysed using a variety of approaches. Our results show that equally weighted parsimony and Bayesian methods cluster unrelated longirostrine forms together, producing a topology that conflicts strongly with their stratigraphic distributions. By contrast, applying extended implied weighting improves stratigraphic congruence and removes longirostrine clustering. The resulting topologies resolve the major neosuchian clades, confirming several recent hypotheses regarding the phylogenetic placements of particular species (e.g. *Baryphracta deponiae* as a member of Diplocynodontinae) and groups (e.g. Tethysuchia as non-eusuchian neosuchians). The longirostrine condition arose at least three times independently by modification of the maxilla and premaxilla, accompanied by skull roof changes unique to each longirostrine clade.

ADDITIONAL KEYWORDS: convergence – cladistic analysis – longirostrine morphology – homoplasy – morphological phylogenetics – Crocodylia – vertebrate palaeontology – Crocodyliformes – parsimony analysis.

INTRODUCTION

Crocodylomorpha is a paucispecific clade in modern faunas, which was thought to include only 23 extant species (Oaks, 2011), although recent genetic work has increased this number to at least 25 (Hekkala *et al.*, 2011; Shirley *et al.*, 2018). By contrast, the rich fossil record of Crocodylomorpha indicates that it was previously much more diverse and widespread, with over 600 named species (Alroy *et al.*, 2018). This clade comprises a paraphyletic array of early diverging taxa ('sphenosuchians') and the monophyletic Crocodyliformes (Brochu *et al.*, 2009), with the latter including the three extant crocodylian families. Although extant crocodylians are often referred to as 'living fossils' because of their apparently conservative anatomy (Buckland, 1836; Meyer, 1984), recent studies have demonstrated that Crocodylomorpha exhibited considerable morphological disparity throughout its evolutionary history (Brochu, 2003). Many of the major constituent clades of Crocodylomorpha diverged during the first 100 million years of its evolutionary history and exhibited numerous unique modifications to their ancestral bauplan. Species range from fully terrestrial (Tennant *et al.*, 2016) through amphibious to fully marine (De Andrade & Sayão, 2014) and, although extant forms are exclusively carnivorous (including the piscivorous Gavialidae), some extinct species are suggested to have been herbivorous or omnivorous (Ösi *et al.*, 2007; Sereno & Larsson, 2009; Melstrom & Irmis, 2019). Several species possessed

*Corresponding author. E-mail: sebastian.groh@ucl.ac.uk

unusual snout shapes (Gasparini *et al.*, 2006) from 'pug-nosed' forms such as *Simosuchus* (Buckley *et al.*, 2000) to extremely long- and thin-snouted taxa such as *Dyrosaurus* and the extant *Gavialis*. Body sizes ranged from <1 m, as in the Atoposauridae (Schwarz-Wings *et al.*, 2011), to giant forms such as *Sarcosuchus imperator* de Broin & Taquet, 1966 with body lengths >11 m (Sereno *et al.*, 2001). This morphological and ecological diversity is paralleled by expansions and contractions in geographical ranges that occurred during the Mesozoic and Palaeogene, especially during periods of higher global temperatures, such as the Eocene (Brochu, 2003), as well as marked changes in species richness through time (Mannion *et al.*, 2015). Crocodylian species richness was coupled strongly with peaks in global thermal maxima (Brochu, 2013).

Given the rich fossil record of crocodylomorphs, their morphological and ecological diversity, wide spatiotemporal range and apparent responsiveness to environmental perturbations, it is unsurprising that there has been considerable interest in crocodylomorph evolution, especially in recent years. While substantial progress has been made towards the goal of a robust, well-resolved phylogeny for the group, many problems remain (see below). Disagreements over phylogenetic relationships have impacted negatively upon our understanding of macroevolutionary patterns: for example, within Eusuchia, the geographical origins of both alligatoroids and crocodyloids continue to be widely debated (Brochu, 1999, 2003; Salisbury *et al.*, 2006; Martin & Buffetaut, 2008; Oaks, 2011; Holliday & Gardner, 2012; Martin *et al.*, 2014; Wang *et al.*, 2016).

Neosuchia is a clade within a larger grouping, Mesoeucrocodylia (Fig. 1), which also includes Notosuchia, plus a number of smaller clades and several paraphyletic grades (De Andrade *et al.*, 2011; Pol & Larsson, 2011). Neosuchia was first defined as 'Atoposauridae, Goniopholidae [sic], Pholidosauridae, Dyrosauridae, *Bernissartia*, *Shamosuchus*, and eusuchians' (Benton & Clark, 1988: 27). The most recent, widely accepted definition of Neosuchia (used throughout the text here) is 'all crocodyliforms more closely related to *Crocodylus niloticus* than to *Notosuchus terrestris*' (Sereno *et al.*, 2001: 4). Although this definition results in the inclusion or exclusion of certain groups depending on the preferred phylogenetic topology (such as Thalattosuchia, Sebecia and Dyrosauridae: Martin *et al.*, 2010), it currently contains approximately 480 species according to the Paleobiology Database (PBDB: Alroy *et al.*, 2018). We limit this study to Neosuchia, because this clade represents the majority of the long, intricate evolutionary history of crocodylomorphs, contains the bulk of their species richness and encompasses a wide range of skull morphologies (Fig. 2).

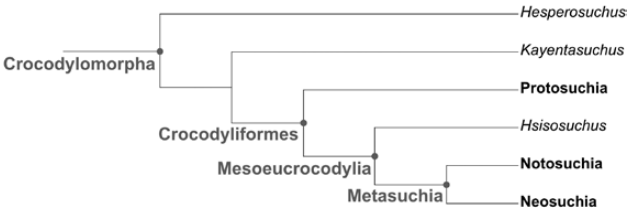

Figure 1. Cladogram of the major crocodylomorph groups, based on Andrade *et al.* (2011), Bronzati *et al.* (2012), and Adams (2014).

The aims of this study are three-fold: (1) to provide a new, comprehensive character list with uniformly worded, clearly defined and illustrated character states for the analysis of neosuchian interrelationships, (2) to identify the analytical approaches that provide the best estimate of neosuchian relationships (e.g. the use of continuous data, extended implied weighting, the application of different tree-building methods, such as maximum parsimony and Bayesian inference) and (3) to investigate patterns of character state assembly and homoplasy during the multiple origins of longirostry in Neosuchia. We start by briefly summarizing current problems in our understanding of neosuchian phylogeny and the difficulties caused by longirostry, and then present our rationale for the assembly and analysis of a comprehensively revised character set. A suite of different analytical protocols are implemented, grounded in theoretical and methodological literature, and the relative accuracy of the resulting tree topologies is assessed by determining their fit to stratigraphy. Finally, we discuss the implications of our results for morphological phylogenetic analyses in general, neosuchian phylogeny and systematics, our understanding of the spatiotemporal distributions of major neosuchian clades and the evolution of the longirostrine condition.

Previous studies of crocodylomorph relationships

The first detailed cladistic analyses of Crocodylomorpha were undertaken during the 1980s (e.g. Clark & Matthew, 1986; Benton & Clark, 1988; Buscalioni & Sanz, 1988). These were followed by further studies that led to analyses with marked increases in character and species numbers, and numerous new phylogenetic hypotheses were proposed during the 1990s and early 2000s (e.g. Norell & Clark, 1990; Gasparini *et al.*, 1991; Clark, 1994; Wu *et al.*, 1994, 1997; Ortega *et al.*, 1996; Gomani, 1997; Brochu, 1999, 2001, 2003; Buckley & Brochu, 1999; Larsson & Gado, 2000; Ortega *et al.*, 2000; Buscalioni *et al.*, 2001; Sereno *et al.*, 2001; Tykoski *et al.*, 2002; Martinelli, 2003; Pol, 2003; Pol & Norell, 2004; Turner, 2004; Jouve *et al.*, 2005). The vast

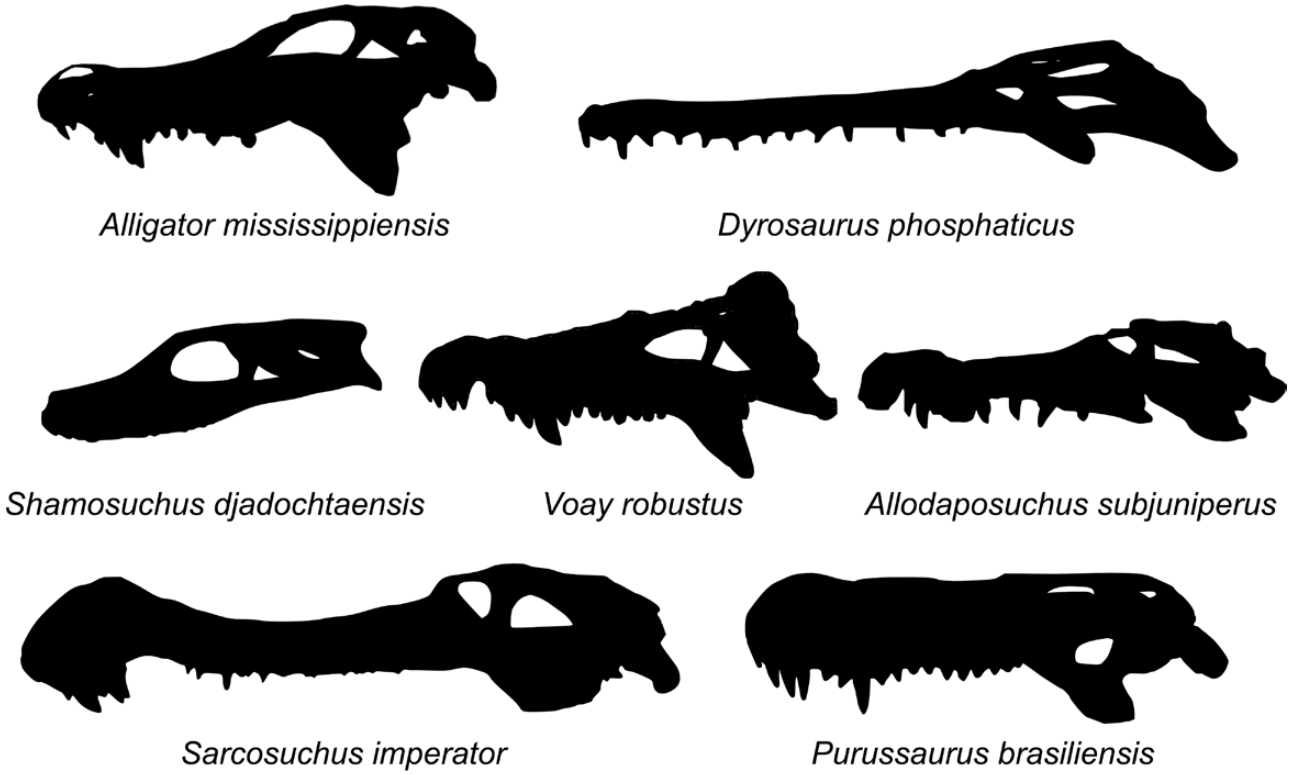

Figure 2. Examples of the morphological diversity of crocodylomorph skulls drawn to the same scale. Ages of the species (following the Palaeobiology Database (PBDB): Alroy *et al.*, 2018). *Alligator mississippiensis*: extant, *Allodaposuchus subjuniperus*: 71–66 Myr, *Dyrosaurus phosphaticus*: 85–49 Myr, *Purussaurus brasiliensis*: 9–7 Myr, *Shamosuchus djadochtaensis*: 85–71 Myr, *Sarcosuchus imperator*: 113–100 Myr, *Voay robustus*: Holocene. Images drawn by the lead author.

majority of subsequent phylogenetic studies derived most of their morphological characters from these earlier works, often without critical re-examination of either the characters or the scores used (e.g. Hill *et al.*, 2008; Lauprasert *et al.*, 2009; Hastings *et al.*, 2010; De Andrade *et al.*, 2011; Puértolas *et al.*, 2011; Holliday & Gardner, 2012; Montefeltro *et al.*, 2013; Turner & Pritchard, 2015; Wilberg, 2015a; Martin *et al.*, 2016a; Wang *et al.*, 2016; Wu *et al.*, 2018). Table 1 presents an overview of selected crocodylomorph phylogenetic studies, illustrating the increase in taxon and character sampling over time.

Within Neosuchia, the affinities of various taxa remain unclear, despite the large number of studies available (Fig. 3). This includes the positions of early diverging non-eusuchians (such as *Bernissartia* and *Mahajangasuchus*: Lauprasert *et al.*, 2009; De Andrade *et al.*, 2011) and eusuchians (such as *Hylaeochampsa* and *Allodaposuchus*: Buscalioni *et al.*, 2011). The placements of *Boverisuchus* and *Borealosuchus* are also contested. *Boverisuchus* is often associated with either Crocodylia (Bronzati *et al.*, 2012) or Planocraniidae (Brochu, 2013). The position of *Borealosuchus* is unclear in its relation to Gavialoidea, being resolved either as the sister-taxon of the latter (Buscalioni *et al.*, 2011; Puértolas *et al.*, 2011) or outside Crocodylia (Bronzati *et al.*, 2012).

An attempt has been made to generate a consensus of these studies using a supertree meta-analysis (Bronzati *et al.*, 2012). Although supertrees can be useful tools for integrating previous phylogenies, this approach has been criticized because robust methods to test these trees are lacking and their topologies might be strongly influenced by the potential non-independence of the source trees (Gatesy & Springer, 2004; Haeseler, 2012). In addition, taxa with uncertain phylogenetic affinities, such as *Borealosuchus* (as mentioned above), can be placed in 'compromise' positions in the supertree as a result of widely differing placements in the source trees.

The phylogenetic studies listed in Table 1 are also potentially problematic in terms of character sampling, construction and treatment. For example, all previous analyses have discretized quantitative characters rather than treating them as continuous data. Furthermore, many previous datasets contain multiple examples of suboptimally constructed characters, such as complex multistate composite characters (see

Table 1. Selected previous studies of crocodylomorph phylogeny. *Bronzati *et al.* (2012) constructed a supertree, rather than using a character-based matrix

Authors	Clade	Number of taxa	Number of characters
Clark (1994)	Crocodyliformes	39	101
Brochu (1999)	Crocodylia	69	164
Sereno *et al.* (2001)	Mesoeucrocodylia	20	72
Wu *et al.* (2001)	Crocodyliformes	32	131
Pol & Norell (2004)	Crocodyliformes	44	183
Jouve *et al.* (2006)	Crocodylomorpha	47	234
Salisbury *et al.* (2006)	Crocodylia	46	176
Hill *et al.* (2008)	Dyrosauridae	14	39
Jouve (2009)	Crocodyliformes	75	143
Hastings *et al.* (2010)	Dyrosauridae	16	82
De Andrade *et al.* (2011)	Crocodylomorpha	104	486
Brochu *et al.* (2012)	Eusuchia	96	179
Bronzati *et al.* (2012)*	Crocodyliformes	184	-
Montefeltro *et al.* (2013)	Neosuchia	90	484
Adams (2014)	Crocodyliformes	90	301
Turner & Pritchard (2015)	Crocodyliformes	101	318
Lee & Yates (2018)	Crocodylia	117	278

below). Composite characters should be atomized and converted into several binary characters, according to Wilkinson (1995), Sereno (2007) and Brazeau (2011), although care has to be exercized with assumptions of character independence (Wilkinson, 1995; Vogt, 2018) and an increase in inapplicable scores (analytically equivalent to increased missing data), resulting from reductive character construction (Maddison, 1993; Strong & Lipscomb, 1999; Seitz *et al.*, 2000). Finally, many characters have been proposed without their individual states being clearly illustrated: given the potential subjectivity of scoring these characters, this lack of clarity is likely to have led to inconsistent scoring of the same character in different analyses. Therefore, a detailed examination and re-evaluation of the available characters for elucidating crocodylomorph phylogeny is long overdue.

THE 'LONGIROSTRINE PROBLEM'

One of the major problems in neosuchian phylogenetics is posed by the evolution of longirostrine taxa: several species, such as members of Tethysuchia, Gavialoidea and Tomistominae, possess markedly thin, elongated snouts, which are regarded as potential adaptations to piscivory (Iordansky, 1973). This superficial similarity between taxa can cause artificial clustering of longirostrine species into clades whose branching patterns are incongruent with their stratigraphic records (Clark, 1994; Jouve, 2009; Meunier & Larsson, 2016), although molecular evidence supports a sister-taxon relationship for the extant longirostrine species *Gavialis* and *Tomistoma* (Roos *et al.*, 2007; Piras *et al.*, 2010). Several methods have been suggested to deal with this problem, including the removal of some longirostrine groups to explore the position of other longirostrine clades (Martin *et al.*, 2016b) and the a priori deletion of characters associated with the longirostrine condition, combined with the removal of several longirostrine taxa from the analysis to avoid artificial associations (Jouve, 2009). Despite the strong homoplastic signal in characters associated with the longirostrine condition, they still retain potential phylogenetic information and, ideally, should not be totally discarded. Although a priori deletion of taxa might remove some of the confounding homoplastic signal, it is also likely to simultaneously reduce the representation of genuinely informative character states.

One method to deal with problems of homoplasy is Implied Weighting (Goloboff, 1993), which is an addition to the maximum parsimony methods based on Farris (1969). It allows the retention of potentially homoplastic characters throughout an analysis, downweighting them to different extents, depending on a preset penalty factor (k) and the distribution of states across the trees being 'considered' during the analysis. An improved version of the algorithm, Extended Implied Weighting ('EIW'), is able to cope better with missing data (Goloboff, 2014). However, O'Reilly *et al.* (2016, 2018b) and Puttick *et al.* (2017) stated that Implied Weighting performed worse than equal-weights parsimony and Bayesian models (see also: Congreve & Lamsdell, 2016). In contrast, Goloboff *et al.* (2017) argued that EIW outperforms all other

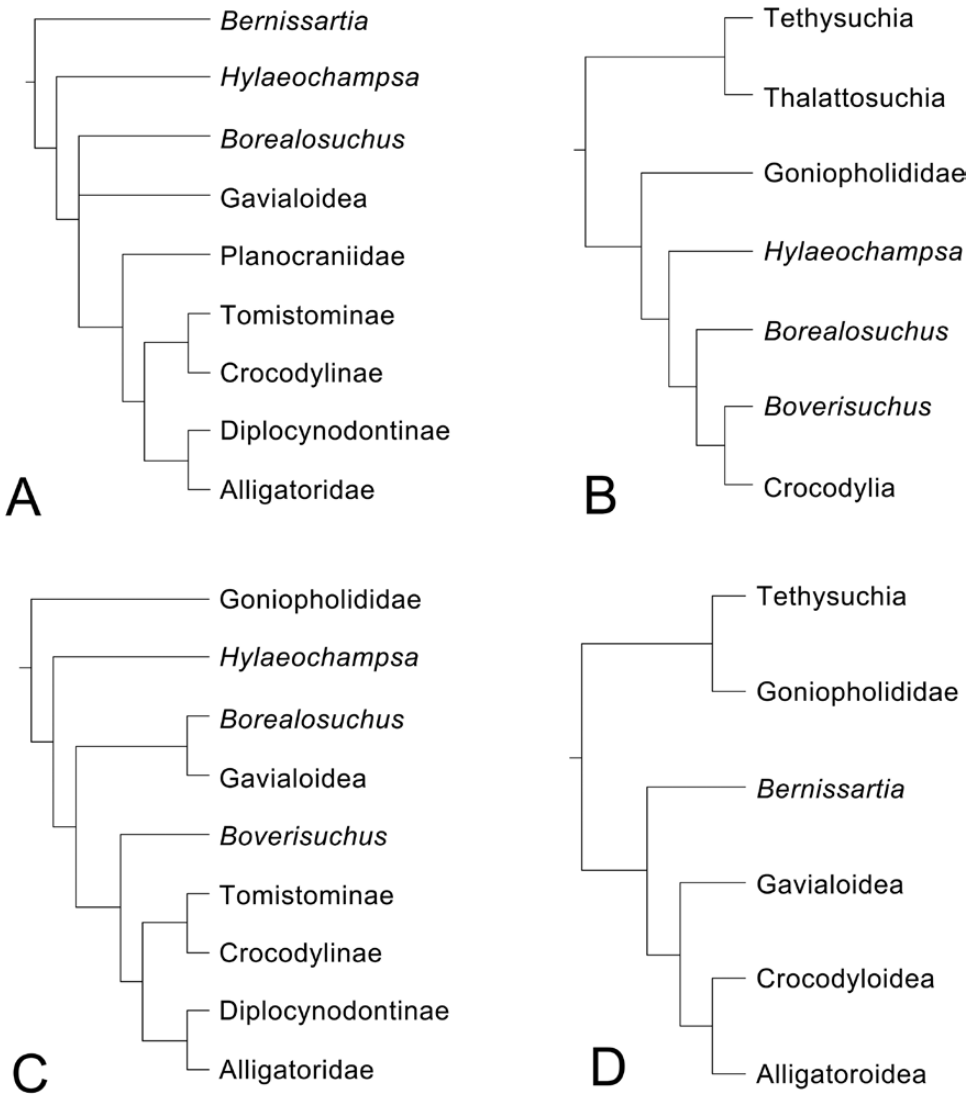

Figure 3. Summary of competing hypotheses of neosuchian and eusuchian phylogenetic relationships. The topologies shown are based on the following analyses: A, Brochu (2013); B, Bronzati *et al.* (2012); C, Buscalioni *et al.* (2011) and Puértolas *et al.* (2011); D, Sereno & Larsson (2009).

methods, including Bayesian analyses, and parsimony has been found to yield more stratigraphically congruent results than Bayesian analyses (Sansom *et al.*, 2018). Despite the recent debate over the effectiveness of weighted parsimony vs. Bayesian analyses and their usefulness in dealing with homoplasy, neither has been applied extensively to neosuchian phylogenetics. Here, we apply both methods in an attempt to tackle 'the longirostrine problem'.

Phylogenetic abbreviations

CI, Consistency Index; EIW, Extended Implied Weighting; GER, Gap Excess Ratio; MPT(s), Most Parsimonious Tree(s); MP, Maximum Parsimony; MSM*, Manhattan Stratigraphic Measure; NTS, New Technology Search; OTU, Operational Taxonomic Unit; RCI, Relative Completeness Index; RI, Retention Index; TL, Tree Length.

Anatomical abbreviations

An, angular; Ar, articular; At, atlas; Ax, axis; Bso, basioccipital; D, dentary; Ecp, ectopterygoid; Exo, exoccipital; F, frontal; Fe, femur; Hu, humerus; Il, ilium; J, jugal; L, lacrimal; Mc, metacarpal; Mx, maxilla; N, nasal; Na, neural arch; Ocn, occipital condyle; Pa, palatine; Par, parietal; Pf, prefrontal; Pi, pisiform; Pmx, premaxilla; Po, postorbital; Pt, pterygoid; Q, quadrate; Qj, quadratojugal; Ra, radius; Ral, radiale; Sa, surangular;

Sp, splenial; Spo, supraoccipital; Sq, squamosal; Ul, ulna; Ulr, ulnare; Vce, vertebral centrum.

Institutional abbreviations

AMNH, American Museum of Natural History, New York, USA; IRScNB, Institut Royal des Sciences Naturelles de Belgique, Brussels, Belgium; IVPP, Institute of Vertebrate Paleontology and Paleoanthropology, Beijing, China; LDUCZ, Grant Museum of Zoology, University College London, UK; MNHN, Museum National d'Histoire Naturelle, Paris, France; NHMUK, Natural History Museum, London, UK; SMNK, Staatliches Museum für Naturkunde Karlsruhe, Karlsruhe, Germany; SMNS, Staatliches Museum für Naturkunde Stuttgart, Stuttgart, Germany; USNM, United States National Museum, Smithsonian Institution, Washington, DC, USA; YPM, Peabody Museum of Natural History, Yale University, New Haven, USA.

MATERIAL AND METHODS

Data collection

A total of 112 neosuchian taxa were included in this study. Morphological characters were scored first-hand from 152 specimens representing 108 taxa, with a further four taxa (*Iharkutosuchus makadii* Ösi *et al*., 2007, *Isisfordia duncani* Salisbury *et al*., 2006, *Koumpiodontosuchus aprosdokiti* Sweetman *et al*., 2015 and *Pietraroiasuchus ormezzanoi* Buscalioni *et al*., 2011) scored from descriptions in the literature.

As outgroup choice has been shown to influence taxon placement in crocodylomorph analyses (Wilberg, 2015a), multiple species outside Neosuchia were selected (N = 8, counting Thalattosuchia), with *Protosuchus richardsoni* Brown, 1933 set as the outgroup to all other taxa (TNT only allows a single outgroup to be designated). A further four non-neosuchians were included (*Araripesuchus gomesii* Price, 1959, *Comahuesuchus brachybuccalis* Bonaparte, 1991, *Notosuchus terrestris* Woodward, 1896 and *Sebecus icaeorhinus* Simpson, 1937), because they represent a range of clades that are currently thought to lie outside Neosuchia, but are more closely related to Neosuchia than *Protosuchus* (Bronzati *et al.*, 2012). In addition, three thalattosuchian species (*Gracilineustes leedsi* Andrews, 1913, *Pelagosaurus typus* Bronn, 1841 and *Steneosaurus bollensis* Cuvier, 1824) are included in the dataset, because Thalattosuchia has been resolved in various positions both in and outside Neosuchia (Benton & Clark, 1988; Wu *et al.*, 2001; Pol & Gasparini, 2009; Young & De Andrade, 2009; Wilberg, 2015a). The analysis also included 19 extant taxa representing all three crocodylian families.

Continuous character measurements were obtained first-hand. Where possible, measurements were taken from multiple specimens of the same species and later entered as ranges in the dataset to minimize collection error, with a maximum of four specimens per species. Only adult specimens were measured, but because crocodylians show little or no sexual dimorphism (Grigg & Gans, 1993), potential differences between males and females were not accounted for.

All measurements and scorings were recorded in Microsoft Office Excel. The ratios between two measurements representing the continuous characters were calculated using Excel, before being transferred into a.tnt file.

Character list assembly and data matrices

An initial character list was assembled following a comprehensive literature search, with characters taken from Brochu (1999), Sereno *et al.* (2001), Wu *et al.*, (2001), Pol & Norell (2004), Jouve *et al.* (2006), Salisbury *et al.* (2006), Hill *et al.* (2008), Jouve (2009), Hastings *et al.* (2010), Montefeltro *et al.* (2013) and references therein. These characters were traced back to their original descriptions and new characters were added based on personal observations and a survey of the more recent literature. Each character was evaluated to establish that it describes unique morphological features, in order to avoid accidental duplication. Each character was re-worded to fit the character construction schemes proposed by Sereno (2007) and Brazeau (2011) to enhance clarity and repeatibility.

After removing obvious duplicates, the original character list contained 1419 discrete characters. All of these characters were checked against specimens of extant crocodylians in the collections of LDUCZ and NHMUK and individually re-evaluated in terms of how accurately they could be replicated and operationalized. This led to the removal of numerous characters for one or more of three major reasons: (1) they represented autapomorphies for OTUs in the dataset and were thus uninformative for resolving neosuchian phylogeny, (2) they were hidden duplicates of other characters, describing the same morphologies but with diferent definitions or (3) they were describing ambiguous morphological variation that could not be applied consistently. A list of these discarded characters, with justifications for their exclusion, can be found in the Supporting Information (S2).

Twenty-three new characters were formulated, nine based on personal observation of specimens and 14 based on features identified in other systematic descriptions (Wu *et al.*, 2001; Brochu, 2007, 2011; Jouve *et al.*, 2008a; Martin *et al.*, 2010, 2014; Buscalioni *et al.*,

2011; Hastings *et al.*, 2013; Skutschas *et al.*, 2014; Turner, 2015).

The original character list contained many complex multistate composite characters. An example of this is character 6 of Pol & Norell (2004: originally from Clark, 1994): 'External nares facing: anterolaterally or anteriorly (0), dorsally not separated by premaxillary bar from anterior edge of rostrum (1), or dorsally separated by premaxillary bar (2)'. According to Sereno (2007) and Brazeau (2011), such characters should be converted into several binary characters. In this case, the two binary characters separate the orientation of the external nares from the presence/absence of the premaxillary bar (see characters 95 and 96 in our character list, available in full as Supporting Information [S1]).

Further problems in character scoring and repeatability have been caused previously not only by unclear wording, but also by the use of character states that are difficult to operationalize; for example, those that employ undefined qualitative terms, such as 'small' and 'large' in lieu of exact state descriptions. Character states using these and other similar terms introduce subjectivity into the analysis and have the potential to affect repeatability. Since evolutionary change often occurs along a continuum rather than via distinct stages (Wiens, 2001) it is more appropriate to convert discretized quantitative characters into continuous ones. Continuous data are less influenced by worker subjectivity (Parins-Fukuchi, 2017) and are a more accurate representation of evolutionary processes that usually occur along a sliding scale rather than in separate, distinct stages (Wiens, 2001). Moreover, continuous characters have been found to have a positive impact on obtaining phylogenies by reducing homoplasy (Jones & Butler, 2018). Such data can now be analysed phylogenetically, using raw measurement data converted into ratios, rather than pre-defined (and often arbitrary) character-state boundaries (Goloboff *et al.*, 2006). Despite problems of covariance (Adams & Felice, 2014; Uyeda *et al.*, 2015), arbitrariness in measurements (Koch *et al.*, 2015) and the potential tendency of placing too much emphasis on general shape, continuous characters have been demonstrated to provide useful phylogenetic information (Wiens, 2001; Goloboff *et al.*, 2006; Jones & Butler, 2018), performing better than discrete characters under certain circumstances, such as under regimes of high evolutionary rates (Parins-Fukuchi, 2017). Here, quantitative characters with arbitrarily defined state boundaries were converted into continuous characters (see: Goloboff *et al.*, 2006) wherever possible, using either the ratio of two clearly defined linear measurements or an angular measurement. If not possible, an effort was made to define distinct states for each character. Several previous studies have employed additional sources of data for neosuchian phylogenetic inference; for example, Piras *et al.* (2010) used a dataset consisting entirely of 3D landmark data from crocodylian skulls, Chamero *et al.* (2014) applied 3D morphometrics to the skull and cervicothoracic region of Crocodylia and Gold *et al.* (2014) used geometric morphometrics to analyse eusuchian braincase structure. However, these studies focused on limited parts of the neosuchian tree.

In order to examine the interdependence and covariance of continuous characters, Principal Components Analysis (PCA) (Brocklehurst *et al.*, 2016) was used with *pcaMethods* (Stacklies *et al.*, 2007) in the R v.3.4.2 environment (R Core Team, 2016). This was applied to all continuous characters and to a subset of ten continuous characters related to the neosuchian longirostrine condition (continuous character numbers 1, 11, 12, 13, 16, 28, 37, 52, 53a and 54a, describing morphological variation usually associated with an elongated, thin snout). The 'longirostrine condition' is defined by us for the purpose of this study by the following two conditions occurring together: (1) the snout length (measured from the anteriormost point of the orbit to the anteriormost point of the skull) being twice as long, or longer, than the remaining skull length (measured from the anteriormost point of the orbit to the posteriormost point of the skull) and (2) a narrow snout whose lateral margins remain parallel for more than half of its length. This corresponds to a ratio of 0.67 or more in character 16 of our character list. For the purposes of the PCA, taxa with more than four missing character states were deleted due to the sensitivity of this method to missing data. NipalsPCA [implemented in the *pcaMethods* package in R, based on an algorithm by Wold (1966)] was used for the analysis of both total continuous data and the longirostrine subset of characters, minimizing the impact of missing data. Analyses were unsuccessful for the complete continuous dataset of 84 characters due to the high proportion of missing information that could not be excluded (>15% missing data). As a result, all characters clustered in the same place in the PCA plots, preventing us from drawing conclusions on character dependency. However, for longirostrine continuous characters only, the results showed a clear clustering of characters 52, 53a and 54a, suggesting that they are not independent from each other. These three characters are as follows: 'skull proportions: ratio of maximum skull width in dorsal view: ratio of maximum skull length in dorsal view' (character 52, new); 'anterior portion of mandible, proportions: ratio of mandible width at anterior end in dorsal view to mandible width close to posterior end of symphysis in dorsal view' [character 53a; after Sereno *et al.* (2001), character 72, modified in Hastings *et al.* (2010), character 70]; 'mandibular symphysis, proportions: ratio of maximum

height of mandibular symphysis to maximum length of mandibular symphysis [character 54a; after Jouve *et al.* (2005, 2008a), character 17]. The original characters 53a and 54a were, therefore, excluded and are marked as such in the full character list.

The final morphological character list used as the basis for our subsequent analyses contains 569 characters (487 discrete and 82 continuous) and is available in the Supporting Information (S1). To facilitate the use of this character list, 163 characters have been illustrated in order to enhance clarity and repeatability of character-state scoring in future analyses. A second version of the full dataset was generated with all continuous characters rediscretized into separate states according to their original character descriptions, in order to evaluate the influence of the alternative treatments of quantitative characters (i.e. continuous data vs. discretized versions) on phylogenetic reconstruction. The full.tnt files of both datasets are available in the Supporting Information (S4).

Data transformations and character settings

In order to ensure that continuous characters were weighted equally in proportion to discrete characters, each character was set to have an initial weight of 100. This is because it is necessary to adjust the relative weights of quantitative characters when expressed as continuous data (e.g. ratios) (Goloboff *et al.*, 2006). The weightings of continuous characters were then adjusted as follows: (1) the total range of the continuous character value was calculated for each character, e.g. 0.5 for character X with values ranging from 0.2 to 0.7; (2) 1 was divided by said total range to obtain a weighting factor, in the case of character X this would be 2; (3) since the initial character weight is 100, the weighting factor was multiplied by 100 to obtain a unique weight for each continuous character (e.g. 200 in the case of character X).

These unique weights were entered manually into the.tnt file to adjust all weightings. In addition, 40 of the 57 discrete multistate characters were treated as ordered because their states represent potential transformation series (Brazeau, 2011): 86, 87, 92, 108, 120, 122, 125, 152, 155, 178, 188, 190, 193, 211, 217, 241, 247, 254, 265, 274, 285, 288, 363, 394, 400, 415, 416, 425, 443, 461, 483, 490, 508, 522, 527, 530, 547, 549, 551 and 552. These ordered characters are also marked in the full character list in the Supporting Information (S1).

Phylogenetic analyses

Maximum parsimony (MP) analyses were performed in TNT v.1.5 (Goloboff & Catalano, 2016). Phylogenies were generated from the different datasets described above, with and without the use of extended implied weighting (EIW) (Goloboff, 2014) in TNT. We used New Technology Search (NTS) with sectorial searches, ratchet, drifting and tree-fusing algorithms enabled on their default settings. The consensus was required to stabilize at least five times with factor 75 before completing the search. The optimal topologies found by these initial new technology searches were then used as starting trees for a traditional TBR search, following the protocol outlined by Mannion *et al.* (2013). For extended implied weighting, analyses were carried out with two different k-values, $k = 3$ and $k = 12$. $k = 3$ represents the standard setting for TNT, while $k = 12$ was recommended as a potentially better alternative by Goloboff *et al.* (2017), as it does not downweight putative homoplastic characters as strongly as lower k-values and produces more accurate trees in a modelled environment.

In addition to unconstrained analyses, we also performed a MP+EIW analysis of the complete dataset using a backbone topological constraint. This backbone (Fig. 4) reflects the currently accepted consensus on neosuchian phylogeny (based on morphology), as found in Brochu (2011) and Bronzati *et al.* (2012). The constrained analysis was carried out to compare our new phylogenetic trees with established hypotheses. Statistical comparison of the lengths of unconstrained and constrained MPTs was carried out using a Templeton test (Templeton, 1983) via the *Templetontest.run* script by Alexander N. Schmidt-Lebuhn (*phylo.wikidot.com/tntwiki*).

In order to identify unstable taxa and the characters responsible for their instability, we applied the command pcrprune (Goloboff & Szumik, 2015), which is based on the *iterpcr* script by Pol & Escapa (2009).

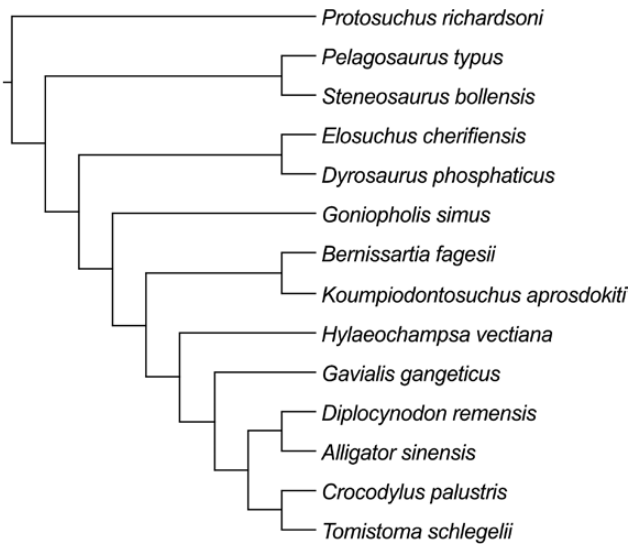

Figure 4. Backbone tree used in the constrained analysis of the complete dataset CW3.

Further analysis of unstable taxa was carried out using RogueNaRok v.1.0 (Aberer *et al.*, 2013). Bremer support was calculated using the script *Bremer.run*, and CI and RI were calculated using the script *Stats.run*, both supplied with TNT. Character statistics were calculated using the *Charstats.run* script by Martin Ramírez, made available online on *sites.google.com/site/teosiste/tp/archivos*. Bootstrap and jackknife supports were generated using NTS with 1000 and 100 replicates, respectively, to avoid excessively high runtime. Character-state mapping was performed using MESQUITE v.3.2 (Maddison & Maddison, 2017).

We also performed Bayesian inference using MrBayes v. 3.2 (Ronquist & Huelsenbeck, 2003; Ronquist *et al.*, 2012). Because MrBayes does not allow for the use of continuous variables, only the rediscretized version of the dataset was analysed via this method. The dataset was analysed using the following commands: lset nst = 1 rates = gamma (denoting the use of the GTR model [nst = 1] and proper analysis of morphological character data, which usually display gamma-shaped variation, see Ronquist *et al.* [2012]) and mcmc ngen = 1000000 samplefreq = 10000 printfreq = 10000 diagnfreq = 10000. After the initial number of 1 000 000 generations, the standard deviation (SD) still proved too high (above 0.01). The SD never dropped below 0.2 so the analyses were stopped after 10 000 000 generations, with a burn-in of 1 000 000.

Stratigraphic congruence

We used stratigraphic congruence as an independent measure to compare different tree topologies. In accordance with the findings of Pol *et al.* (2004), we did not employ statistical tests between the different support measures, and only compared tree topologies based on the same species sets. Stratigraphic congruence for each of the resulting trees was calculated using the package *strap* (Bell & Lloyd, 2014) in the R environment, applying the command StratPhyloCongruence with 1000 permutations each for resampled and randomly generated trees. Taxon ages were taken from the PBDB (Alroy *et al.*, 2018) and adjusted to be congruent with the International Chronostratigraphic (ICS) chart (Cohen *et al.*, 2013) and any updates based on the recent literature, and are listed in full in the Supporting Information (S4). For those taxa with only one occurrence in the fossil record, uncertainties in dating were taken into account by using the midpoint ages of their inferred stratigraphic ranges. Several taxa, such as *Dyrosaurus phosphaticus* Thomas, 1893, displayed genuine stratigraphic ranges with multiple occurrences in the fossil record and were entered into the ages file as such.

Stratigraphic congruence was calculated using three metrics: Relative Completeness Index (RCI) (Benton & Storrs, 1994), Manhattan Stratigraphic Measure (MSM*) (Siddall, 1998; Pol & Norell, 2001) and Gap Excess Ratio (GER) (Wills, 1999). The RCI is based on the ratios between the observed age ranges of taxa with the lengths of their inferred ghost ranges (i.e. the remaining branch lengths of the tree). Thus, it functions similarly to a completeness metric, by determining how much of a total branch length of the time-scaled tree can be explained by actual taxon ranges. MSM* is based on similar algorithms to the character consistency index (Kluge & Farris, 1969) where the ages of terminal taxa are represented as Sankoff characters. In contrast to RCI, it compares a hypothetical tree with optimal stratigraphic congruence to the congruence of a given tree's topology. The GER is similar to MSM* in that it operates with a hypothetical tree of best stratigraphic congruence and topology of a given tree. However, it also takes into account suboptimal trees and calculates stratigraphic congruence with optimal and suboptimal tree topologies compared to the target tree that is being tested for stratigraphic congruence.

RESULTS

For ease of reference and discussion throughout, our various phylogenetic analyses are here referred to via a simple system of abbreviations (see Table 2).

Table 2. Tree statistics for the six parsimony analyses. CI, Consistency Index; EIW, Extended Implied Weighting; MPTs, Most Parsimonious Trees; RI, Retention Index; TL, Tree length

Abbreviation	Dataset	Method	EIW	*k*-value	No. of MPTs	TL	CI	RI
C	Complete	Maximum Parsimony			8	234374.2	0.261	0.599
CW3	Complete	Maximum Parsimony	x	3	3	244245.9	0.250	0.576
CW12	Complete	Maximum Parsimony	x	12	2	236243.3	0.259	0.595
R	Rediscretized	Maximum Parsimony			99999+	2346	0.252	0.6
RW3	Rediscretized	Maximum Parsimony	x	3	6	2444	0.242	0.578
RW12	Rediscretized	Maximum Parsimony	x	12	12	2363	0.251	0.596

PHYLOGENETIC ANALYSES

The results of the tree searches (Table 2) generally fall into three different categories (Fig. 5): (1) topologies where the longirostrine groups are clustered together (analyses without EIW, and with EIW under $k = 12$), (2) topologies where the longirostrine groups are resolved as distinct clades in different positions (analyses with EIW and $k = 3$) and (3) topologies whose strict consensus trees are characterized by numerous polytomies (Bayesian analysis, rediscretized dataset without EIW).

Taxon pruning and the use of RogueNaRok (Aberer *et al.*, 2013) yields limited and unclear results as tree resolution is not significantly improved following the removal of potential 'rogue' taxa. Only a handful of taxa are shown to affect consensus tree resolution when removed. These taxa are either members of Tethysuchia (*Dyrosaurus*, *Rhabdognathus* and *Pholidosaurus*) or Crocodyloidea (*Crocodylus affinis*, *C. elliotti*, *C.* cf. *clavis* and *C. megarhinus*), in which all taxa of the latter clade have similar scores. A full list of apomorphies for each node in the unconstrained tree topology of the complete dataset analysis can be found in the Appendix.

STRATIGRAPHIC CONGRUENCE

The trees resulting from analysis CW3 (complete dataset with EIW and $k = 3$) yield the best results with respect to stratigraphic congruence (with RCI values above –300 for the unconstrained, and ranging from –296 to –312 for the constrained analysis MPTs), followed by RW3 (rediscretized dataset with EIW and $k = 3$) (RCI > -400) (see Table 3). In both cases, changing the k-value from 3 to 12 results in worse stratigraphic

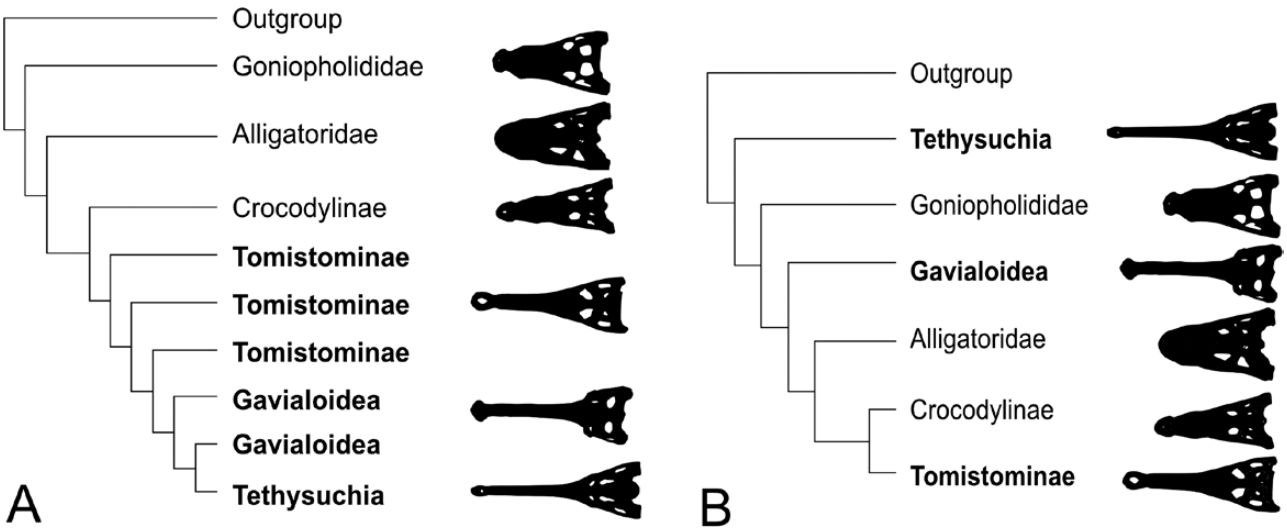

Figure 5. Illustration of the two major tree topologies obtained. The analyses yielded the following topologies in their strict consensus trees: A, unweighted analyses B, analyses using extended implied weighting with $k = 3$. Outlines drawn by the lead author.

Table 3. The results of the stratigraphic congruence analyses for each parsimony and Bayesian analysis performed. EIW, Extended Implied Weighting; GER, Gap Excess Ratio; MSM, Manhattan Stratigraphic Measure; RCI, Relative Completeness Index. The p-values for all stratigraphic congruence values (not shown) were all $P < 0.05$

Abbreviation	Dataset	Method	EIW	*k*-value	RCI		GER		MSM*	
					Best tree	*Worst tree*	*Best tree*	*Worst tree*	*Best tree*	*Worst tree*
C	Complete	Maximum Parsimony			-589	-606	0.728	0.721	0.046	0.045
CW3	Complete	Maximum Parsimony	x	3	-273.8	-275.7	0.859	0.858	0.085	0.085
CW12	Complete	Maximum Parsimony	x	12	-610.8	-611.8	0.719	0.719	0.045	0.045
R	Rediscretized	Maximum Parsimony			-540.5	-729.5	0.748	0.670	0.050	0.038
RW3	Rediscretized	Maximum Parsimony	x	3	-329.1	-365.6	0.836	0.821	0.074	0.068
RW12	Rediscretized	Maximum Parsimony	x	12	-670.9	-694.4	0.694	0.685	0.041	0.040
RB	Rediscretized	Bayesian Inference			-768.3	-1020.8	0.654	0.556	0.037	0.029

congruence (RCI ranging from –610 to –695). The trees obtained from analyses C (complete dataset with equal weights parsimony) and R (rediscretized dataset with equal weights parsimony) and those trees resulting from analysis RB (rediscretized dataset with Bayesian statistics) yield considerably worse stratigraphic congruence values, with RCI ranging from –540 to –730 and –768 to –1020, respectively (Table 3).

Topological details

Analyses C, R and RB result in clustering of most longirostrine taxa. In contrast, analyses CW3 and RW3 result in all major longirostrine clades appearing in distinctly separate regions of the tree. However, individual lineages and subclades differ greatly in their positions or internal structure. The results of the Templeton test show that the trees resulting from the constrained version of analysis CW3 are not significantly worse explanations of the data than those generated by the unconstrained analysis of CW3.

Araripesuchus, *Comahuesuchus* and *Notosuchus* are consistently resolved as a monophyletic notosuchian outgroup, associated with *Shamosuchus*, *Theriosuchus* and *Sebecus*. Thalattosuchia and Tethysuchia are paraphyletic in the results of analyses CW3 and RW3, although the relationship between taxa varies between analyses. All thalattosuchian taxa are consistently resolved as outgroups to Neosuchia. *Hyposaurus*, *Congosaurus*, *Dyrosaurus* and *Rhabdognathus* form an unresolved monophyletic group in analyses CW3 and RW3 (Fig. 6), and *Elosuchus*, *Sarcosuchus* and *Pholidosaurus* occur in various positions in the trees [see Supporting Information (S3)].

Susisuchus anatoceps Salisbury *et al.*, 2003 is consistently placed as the closest sister-group to Goniopholididae in analyses CW3 and RW3 (Fig. 6). *Sunosuchus* and *Vectisuchus* are included in Goniopholididae in analysis RW3. They are placed as sister-taxa to Goniopholididae in the unconstrained version of CW3.

In all weighted analyses, *Bernissartia fagesii* Dollo, 1883 is consistently found as the sister-taxon to all Eusuchia (Fig. 6). However, the clade including *Hylaeochampsa* is resolved as the sister-group to Brevirostres (Crocodyloidea + Alligatoroidea), except for the constrained version of CW3 where the backbone tree forces it to be the sister-group to the remaining eusuchians.

Analyses CW3 and RW3 yield monophyletic Gavialoidea and Gavialinae with similar species compositions, although with slight differences in internal relationships. *Maroccosuchus zennaroi* Jonet & Wouters, 1977 is resolved in Gavialoidea in CW3 (Fig. 6), but as part of Tomistominae in RW3. Both place *Tomistoma dowsoni* Fourtau, 1918 in Gavialoidea.

In addition, Crocodyloidea and Alligatoroidea are monophyletic in analyses CW3 and RW3. However, the greatest difference lies in the position of Diplocynodontinae: CW3 resolves it as the sister-group to Crocodylia, whereas RW3 places it as the sister-group to Alligatoridae, as is also enforced in the constrained version of analysis CW3. In addition, the position of the two species of *Planocrania* varies markedly between CW3 and RW3: as sister-group to Diplocynodontinae (RW3) or sister-group to Crocodylidae (CW3) (Fig. 6). Similarly, *Eoalligator chunyii* Young, 1964 is resolved in different positions, as either the sister-group to the remaining Brevirostres (CW3) or more deeply nested within Alligatoridae (RW3). *Leidyosuchus canadensis* Lambe, 1907 and *L. gilmorei* Mook, 1842 are placed either as the sister-group to all remaining Alligatoridae (RW3) or Diplocynodontinae (CW3). Both CW3 and RW3 show a paraphyletic Alligatorinae (with slightly different internal relationships) and monophyletic Caimaininae.

Tomistominae is consistently placed within Crocodylidae, as the sister-group to Crocodylinae, although the internal relationships of Crocodylinae vary across different analyses, especially with respect to the positions of *Crocodylus siamensis* Schneider, 1801 and *C. novaguineae* Schmidt, 1928.

Support values

Support values for the trees stemming from analysis CW3 are low overall, with few groups receiving high support for any of the three measures used (bootstrap, jackknife and Bremer). The best-supported groups for CW3 include: *Notosuchus* and *Comahuesuchus* (bootstrap = 97, jackknife = 98), the two species of *Eosuchus* (bootstrap = 77, jackknife = 72) and the two species of *Planocrania* (bootstrap = 74, jackknife = 85). See Figure 6 for all support values.

DISCUSSION

Methodological implications

Extended implied weighting

Extended implied weighting with $k = 3$ consistently yielded results with better stratigraphic congruence than the same dataset analysed without EIW or with $k = 12$, a pattern repeated across all datasets (Table 3). Higher stratigraphic fit does not always reliably indicate accurate phylogenetic position (Smith, 2000; Geiger *et al.*, 2001). Therefore, it is used here as an auxiliary criterion, independent of phylogeny, thus providing some basis for selecting between alternative topologies (as seen in: Ausich *et al.*, 2015; Randle & Sansom, 2017). The

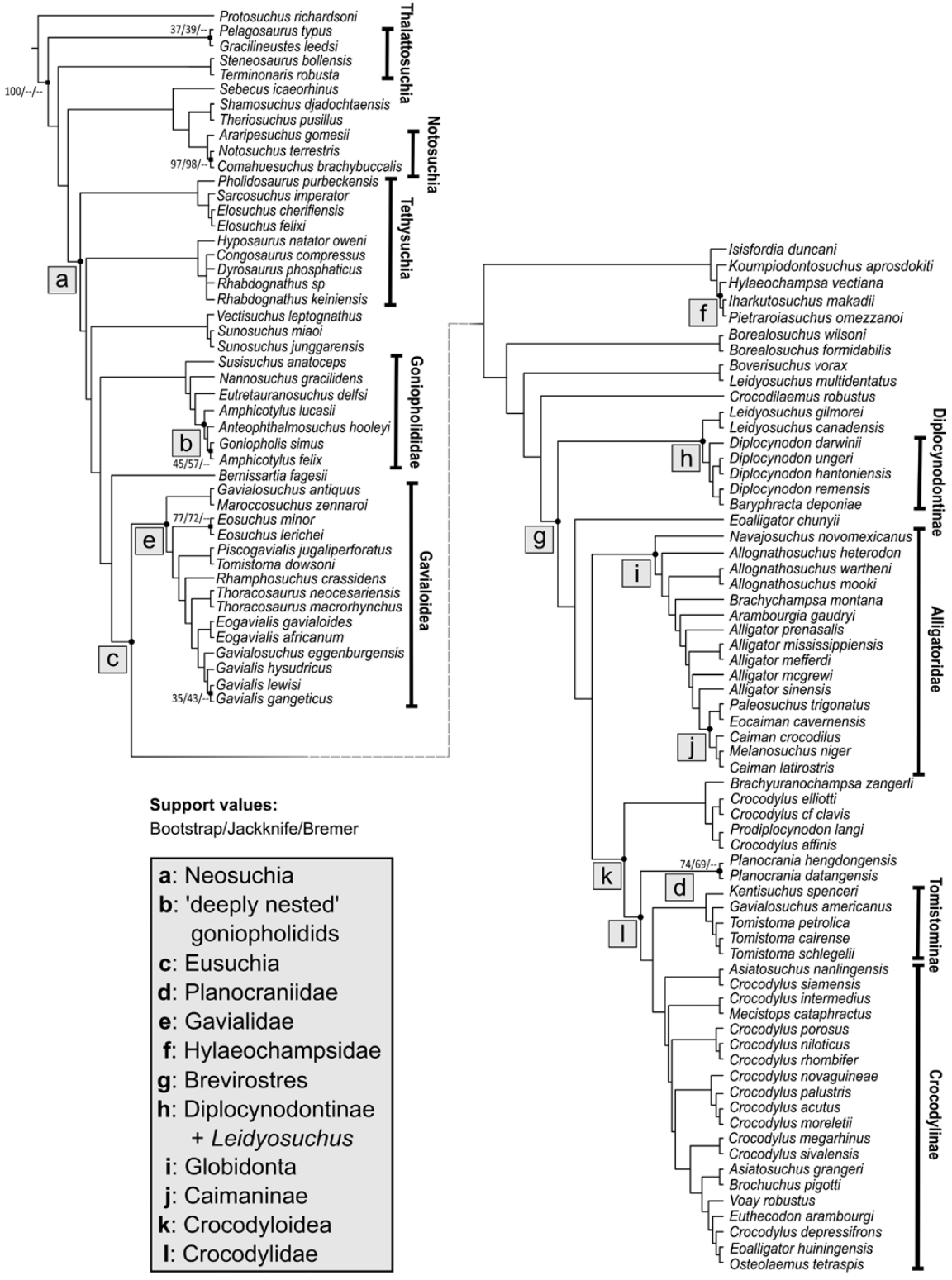

Figure 6. Strict consensus tree obtained by the unconstrained extended implied weights analysis of the complete dataset CW3 with $k = 3$. Support values are in the following order: Bootstrap/Jackknife/Bremer value.

largescale differences in the stratigraphic congruence values seen in our results, in conjunction with the non-clustering of longirostrine taxa, clearly suggest that the CW3 and RW3 trees represent a substantial improvement when compared to the C, R, CW12, RW12 and RB phylogenies. All analyses using EIW with $k = 3$ (CW3 and RW3) resolved Thalattosuchia, Tethysuchia, Gavialoidea and Tomistominae as separate longirostrine clades. The same datasets analysed without EIW (C, R, RB) or EIW and $k = 12$ (CW12, RW12) often yielded a single clade clustering all long- and slender-snouted taxa [for the different topologies see Supporting Information (S3); Fig. 5]. This extreme clustering of longirostrine taxa could stem from the use of continuous data (see below), with the use of EIW negating their effect. However, the rediscretized dataset analysed without EIW (R) exhibits the same pattern of clustering [see Supporting Information (S3)]. It is apparent that the usage of EIW with a low k-value plays a key role in obtaining trees whose topologies are less determined by homoplastic features, such as those associated with convergent instances of snout elongation.

Despite Goloboff *et al.* (2017) arguing for the use of higher k-values (with $k = 12$ given as the optimum), our results for those analyses conducted with lower k-values display higher stratigraphic congruence. Both the complete and rediscretized datasets analysed with $k = 3$ (RCI –273.8 to –275.7 and –329.1 to –365.6, respectively) yielded more stratigraphically congruent trees than those analysed with $k = 12$ (RCI –610.8 to –611.8 and –670.9 to –694.4, respectively) (Table 3). The latter trees once again clustered longirostrine species together. This result reflects a high degree of homoplasy, either caused by the addition of continuous characters to the new dataset, or in neosuchian evolution as a whole (introduced as strong secondary signal by snout shape), since lower k-values are known to downweigh homoplastic characters more strongly (Goloboff *et al.*, 2017). Here, we suggest that the latter explanation (i.e. that EIW has successfully identified and mitigated a homoplasy-driven secondary signal) is better supported, especially given other recent evidence that the treatment of quantitative characters as continuous data tends to reduce homoplasy (Jones & Butler, 2018).

Parsimony is the most commonly used method in reconstructing phylogenies using morphological data, although it has been argued that this is due to force of habit rather than the selection of the best method available (Congreve & Lamsdell, 2016). Recent debate has questioned the usefulness of parsimony in phylogenetic reconstruction in comparison with Bayesian methods and whether one outperforms the other (see: Wright & Hillis, 2014; O'Reilly *et al.*, 2016, 2018a, 2018b; Goloboff *et al.*, 2017; Puttick *et al.*; 2017, Sansom *et al.*, 2018; Yang & Zhu, 2018; Smith, 2019). Our results add to this debate by supporting the utility of EIW when analysing morphological data, particularly in cases where strong homoplasy might overprint the true phylogeny. In contrast, Bayesian analyses of the same datasets produced large numbers of polytomies and trees where longirostrine clades cluster together (representing either hard polytomies and a close relationship between longirostrine taxa, or incorrect tree reconstruction).

Treatment of quantitative characters

The trees obtained by analysing CW3 (the complete dataset, including both continuous and discrete characters, with EIW) yielded consistently higher stratigraphic congruence values for all three measures than those resulting from the rediscretized dataset (Table 3). Without EIW, the stratigraphic congruence values fall within similar ranges for the continuous and rediscretized datasets, both of which show clustering of longirostrine taxa. The use of continuous characters causes general skull shape to play a strong role in tree reconstruction, potentially contributing to the extreme clustering of longirostrine taxa. However, as this clustering is also observed in the analyses without continuous characters (R, RW12 and RB), our results point to improved accuracy in tree reconstruction when using continuous characters in conjunction with EIW.

During the rediscretization of the continuous characters, it became apparent that most of these characters (as deployed in previous studies) had been constructed on the basis of arbitrarily defined boundaries between character states. These arbitrary limits usually did not reflect true differences or gaps in the continuous variation of measurement-based ratios. An example can be seen in Fig. 7, for character 3 [based on character 3 from Hastings *et al.* (2010)]: thickness of anterior margin of external nares in relation to external nares: less than half anteroposterior length (0); same or greater than half anteroposterior length (1). The boundary of 0.5 between the two states does not reflect a clear categorical variation in ratios obtained by measuring a variety of different species. The vast majority of continuous characters in our dataset show similar patterns of non-categorical variation [see continuous character scores in Supporting Information (S4)].

Thus, the combined use of EIW and continuous characters provides a valid alternative to the a priori deletion of potentially homoplastic characters and the possible loss of relevant phylogenetic information that such characters might contain.

Implications for neosuchian phylogeny and systematics

The most stratigraphically congruent tree found in our analyses (Fig. 6, based on CW3) resolved all of the major neosuchian clades proposed by previous

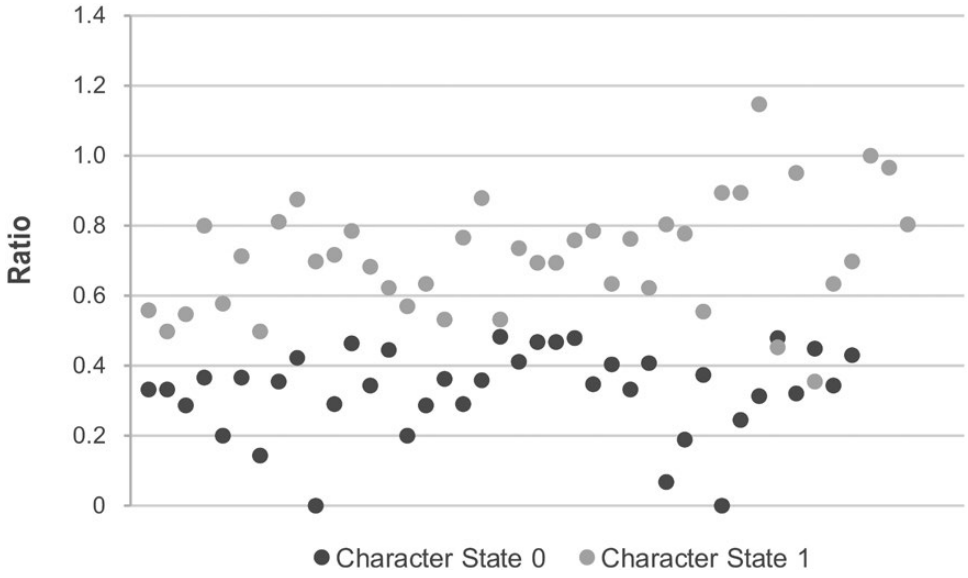

Figure 7. Scatterplot of all the character scores for character 3 in our character list [see Supporting Information (S1)]. Each point represents the obtained ratio for one of our measured specimens (distance between anterior margin of nares and anterior margin of rostrum in dorsal view to maximum anteroposterior length of external nares in dorsal view). Colours mark character scores in the rediscretised version, according to character 3 in Hastings *et al.* (2010): black, character state 0 (anterior margin of external nares less than half of anteroposterior length of external nares; ratio <0.5); grey, character state 1 (anterior margin of external nares greater than half of anteroposterior length of external nares; ratio > 0.5).

phylogenetic studies (for a list of studies see: Table 1). However, it differed from the majority of these in placing Diplocynodontinae as the sister-group to Brevirostres, rather than within Alligatoroidea, as well as resolving Tethysuchia and Thalattosuchia as paraphyletic.

Most of the synapomorphies discussed below are skull and mandible characters, which is unsurprising as the character list is dominated by features in these anatomical regions (77.9% of all characters). Moreover, postcranial material is less frequently (or sometimes never) preserved for many of the species in the dataset.

Tethysuchia

The interrelationships of Tethysuchia have been controversial (De Andrade *et al.*, 2011; Young *et al.*, 2014; Martin *et al.*, 2016b; Meunier & Larsson, 2016; Fig. 8). Our analyses support the placement of Tethysuchia as an early diverging neosuchian clade rather than the alternative position of it being more deeply nested in Eusuchia (*contra* Rogers, 2003).

In addition to being proposed as the sister-clade of Dyrosauridae (Fortier *et al.*, 2011; Young *et al.*, 2014), pholidosaurids have been suggested to be paraphyletic within Tethysuchia (De Andrade *et al.*, 2011), closely related to Goniopholididae (Martin *et al.*, 2016b) or grouped together only by longirostrine characters (Meunier & Larsson, 2016). Our results from analysis CW3 (Fig. 6) clearly refute the latter three hypotheses, as Pholidosauridae is resolved as monophyletic. However, Pholidosauridae is placed as the sister-group of the remaining tethysuchians + remaining Neosuchia in the unconstrained analysis, rendering Tethysuchia paraphyletic as a whole. If analysis CW3 is constrained, it finds Tethysuchia to be monophyletic, although almost all tethysuchians form an unresolved polytomy.

In contrast to the results presented by Young *et al.* (2016), both species of *Elosuchus*/*Fortignathus* are found in Pholidosauridae in our CW3 trees, instead of *F. felixi* as a dyrosaurid. *Elosuchus* is grouped with *Sarcosuchus* and *Pholidosaurus* on the basis of the ventral edge of the premaxilla being situated deeper than that of the maxilla in lateral view (character 112), a zigzag-shaped frontoparietal suture on the interfenestral bar (character 195) and a well-developed anterolateral process on the postorbital (character 200). In contrast to the tree of De Andrade *et al.* (2011), *Elosuchus* does not form a clade with *Vectisuchus*, so we find no support for 'Elosuchidae', despite most of our character scores being similar to those of Andrade *et al.* (2011). In the CW3 tree, *Vectisuchus* forms a clade with the two species of *Sunosuchus* (Fig. 6), outside both Tethysuchia and Goniopholididae [where it was placed by Tykoski *et al.* (2002) and our RW3 analysis].

In addition to supporting a monophyletic Pholidosauridae, our CW3 analysis also resolves

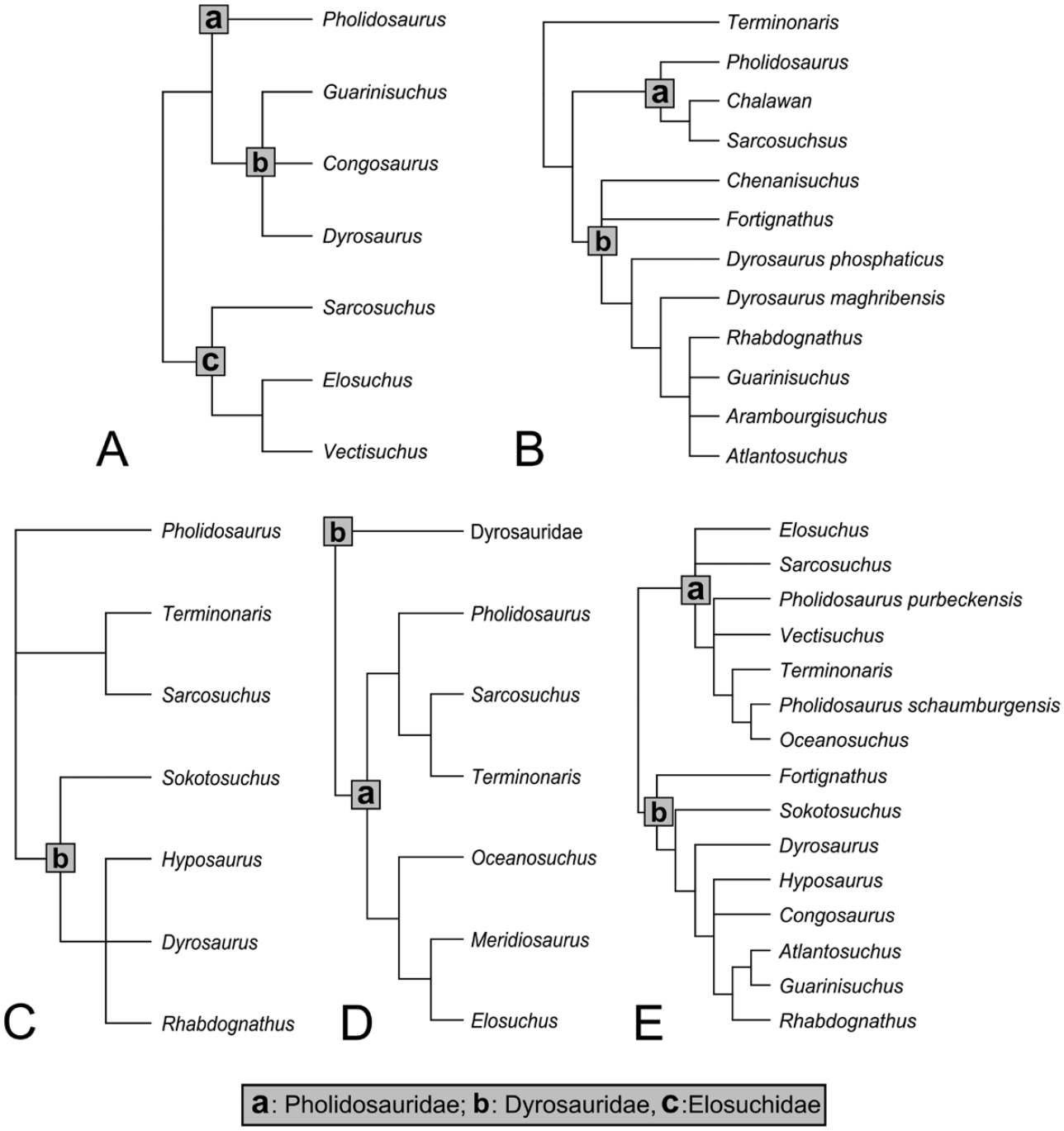

Figure 8. Summary of the competing hypotheses of tethysuchian phylogenetic relationships based on the following analyses: A, Andrade *et al.* (2011); B, Young *et al.* (2014) in Young *et al.* (2016); C, Martin *et al.* (2016b) and Puértolas *et al.* (2011); D, Fortier *et al.* (2011); E, Hastings *et al.* (2010) in Young *et al.* (2016).

Dyrosauridae as monophyletic, supporting the conclusions of Hastings *et al.* (2010) and Martin *et al.* (2016b). However, within this grouping, *Dyrosaurus*, *Congosaurus* and *Rhabdognathus* form a polytomy.

Terminonaris robusta Wu *et al.*, 2001, which is typically classified as a pholidosaurid (e.g. Puértolas *et al.*, 2011; Martin *et al.*, 2016b), groups instead with the thalattosuchian *Steneosaurus bollensis* Cuvier, 1824 (Fig. 8). This relationship might result from the amount of missing data for our examined specimen of *Terminonaris*, as, despite possessing relatively complete skulls, many features were unscorable.

Unstable early diverging neosuchian taxa

In addition to incomplete taxon sampling (covering 105 of 480 neosuchian taxa), which can lead to issues associated with long-branch attraction (Bergsten, 2005), the most prevalent problem in this study, as with many other fossil datasets, is the high proportion of missing data. Our dataset contains 49.7% misssing data, the most complete taxon being *Crocodylus porosus* (7.7% of entries marked with '?', resulting from inapplicable characters) and the most incomplete being *Congosaurus compressus* (extremely fragmentary material with 94.3% missing data). It is possible that this factor has led to varying placements of multiple taxa such as *Shamosuchus djadochtaensis* Mook, 1924 [an early diverging neosuchian according to Pol *et al.* (2009)], *Crocodilaemus robustus* Jourdan, 1857 [a pholidosaur according to Young *et al.* (2011)] and *Theriosuchus pusillus* Owen, 1878 [an early diverging neosuchian recently removed from Atoposauridae by Tennant *et al.* (2016)]. *Shamosuchus* and *Theriosuchus* are resolved as the sister-group of Notosuchia in our CW3 and RW3 analyses, whereas *Crocodilaemus* is placed as the sister-group of Crocodylia (CW3, see Fig. 6) and within Alligatoridae [RW3, see Supporting Information (S3)].

Hylaeochampsidae

Our CW3 and RW3 analyses resolve Hylaeochampsidae in a novel position as the sister-group of Brevirostres (Fig. 6), rather than in its more typical placement as the sister-group of Crocodylia (Buscalioni *et al.*, 2011). In addition, the susisuchids *Isisfordia duncani* and *Koumpiodontosuchus aprosdokiti* (Sweetman *et al.*, 2015; Turner & Pritchard, 2015) are placed as sister-taxa of Hylaeochampsidae in both CW3 and RW3, separate from *Bernissartia*. This association is based on the following characters: concave rostrum contour (character 86); anterior process of frontal truncated (character 182); squamosals extending to orbit margin and overlapping postorbitals (character 227); posterior edge of quadrate gently concave in dorsal view (character 283); paroccipital process dorsolaterally directed at a 45° angle in occipital view (character 290); prezygapophyseal processes of the anterior to middle cervical vertebrae flat or slightly convex (character 487); and a concave surface of the anterior centrum of the first caudal vertebra (character 501).

Goniopholididae and Susisuchus

The phylogenetic relationships of Goniopholididae in the CW3 analysis places a clade consisting of *Vectisuchus* and the two species of *Sunosuchus* as the sister-group to Goniopholididae + the remaining neosuchians (Fig. 6). Previously, these two genera have been identified either as two of the most shallowly nested goniopholidids (De Andrade *et al.*, 2011; also found in the constrained version of analysis CW3) or a more deeply nested goniopholidid in the case of *Sunosuchus* (Martin *et al.*, 2016b; although its placement was not discussed in the latter paper).

One novel aspect of our results is the identification of *Susisuchus anatoceps* as the sister-taxon of Goniopholididae in both our CW3 and RW3 analyses. *Susisuchus* has previously been placed outside Neosuchia (Jouve, 2009) or as part of Susisuchidae at the base of Neosuchia (Fortier & Schultz, 2009; Turner & Pritchard, 2015). The two synapomorphies supporting the association of *Susisuchus* and Goniopholididae in our trees are: dorsal process of premaxillae extending beyond third maxillary alveolus (character 108) and caudal vertebrae with amphicoelous centra from second vertebra onward (character 503).

Borealosuchus *and Planocraniidae*

Our CW3 and RW3 analyses resolves *Borealosuchus* as the sister-taxon of Brevirostres, similar to the results presented in Brochu (2001) (Fig. 6). This is in contrast to Pol *et al.* (2009), where it is one of the earliest diverging eusuchian lineages (Holliday & Gardner, 2012) and formed a polytomy with Gavialoidea; and Puértolas *et al.* (2011), where it was placed as the sister-group to Gavialoidea. Its position as the sister-taxon to Brevirostres in our analyses is based on: alveolar walls raised relative to ventral surface of maxilla (character 131); a weak postorbital bar (its width less than half of the bar height) (character 213); anterior edge of choanae closer to posterior edge of pterygoid flanges than suborbital fenestrae (character 352); and third maxillary alveolus larger in diameter than second alveolus (character 391). Our character scores mostly agree with those in previous studies, but they are overwhelmed by the addition of other characters in our revised dataset.

Planocraniidae *sensu* Brochu (2013), who defined it as consisting of both species of *Planocrania* + *Boverisuchus*, is not identified in any of our analyses. This is despite the fact that our scores include the same apomorphies that grouped the three species together in Brochu (2013): labiolingually compressed teeth on both maxilla and dentary (characters 396 and 414). However, in our analysis, these two characters do not provide a strong enough signal to resolve Planocraniidae. Both CW3 and RW3 analyses place the two *Planocrania* species as the sister-group of Crocodylidae on the basis of the lateral carotid foramen opening dorsal to the basisphenoid lateral exposure (character 318) and parallel to subparallel lateral edges of the anterior half of the interfenestral bar between the suborbital fenestrae (character 366). *Boverisuchus*

is placed as the sister-taxon of Brevirostres, based on: a single projection of the postorbital bar (character 216); the posteriormost maxillary alveolus being closer to the anterior margin of the orbit than the posterior margin (character 394); and dentary teeth occluding lingually to maxillary teeth (character 425).

Gavialoidea

In line with the majority of recent morphological phylogenies (with the notable exception of Halliday *et al.*, 2013), we find Gavialoidea and Tomistominae as separate lineages, with Gavialoidea as the sister-clade of Brevirostres and Tomistominae as the sister-clade of Crocodylinae, nested within Crocodyloidea (Fig. 6).

The overall branching pattern within Gavialoidea is similar in both the CW3 and RW3 analyses and resembles that found in Jouve *et al.* (2015), with the exception of *Piscogavialis jugaliperforatus* Kraus, 1998, which is resolved in an earlier diverging position and forming a clade with *Rhamphosuchus*. The separation of thoracosaurs from Gavialoidea proposed by Lee & Yates (2018) (based on incorporating stratigraphy directly into phylogenetic analysis) is not supported, possibly because our analysis did not incorporate stratigraphic data directly into tree reconstruction and/or because of differences in taxon sampling and character construction and scoring. Instead, our results provide a number of synapomorphies uniting thoracosaurs and gavialoids: large supratempral fenestrae, covering more than 50% of the skull roof surface (character 224); no parietopostorbital suture on dorsal skull roof (character 244); and an anterior notch at the jugal-lacrimal contact, filled by the maxilla (character 250).

Two or three taxa are grouped within Gavialoidea in our CW3 analysis, despite their previous referrals to Tomistominae: *Maroccosuchus zennaroi* Jonet & Wouters, 1977 [an early diverging tomistomine according to Jouve *et al.* (2015) and our RW3 analysis] and two species of *Gavialosuchus* [both tomistomines according to Brochu & Storrs (2012)]. The examined *Maroccosuchus* specimen (IRSNB R408) had limited access and was more fragmentary than other specimens described in the literature. This resulted in several of the characters usually uniting it with Tomistominae (such as the extent of the pterygoid wings and the morphology of the choanae; see Jouve *et al.*, 2015) being scored as unknown, changing the position of *Maroccosuchus* in our CW3 tree. *Gavialosuchus eggenburgensis* Toula & Kail, 1885 (in the unconstrained CW3 and RW3 analyses) and *G. antiquus* Leidy, 1852 are grouped with the Gavialidae + *Thoracosaurus* clade on the basis of: the frontoparietal suture being entirely on the skull table (character 193); barely visible posterior walls of supratemporal fenestrae in dorsal view (character 225); dorsal and ventral rims of groove for external ear valve musculature flaring anteriorly (character 230); parietopostorbital suture present on dorsal skull roof (character 244); no midline crest on basioccipital plate below occipital condyle (character 304); basioccipital with large pendulous tubera (character 305); dentary symphysis extending beyond eighth dentary alveolus (character 400); lateral edges of dentary oriented longitudinally, with convex anterolateral corner and extensive transversely oriented anterior edge (character 401); and distal rami of mandible strongly curved medially at mid-length, giving the mandible a broad 'Y'-shaped outline (character 468).

A third taxon, *Tomistoma dowsoni*, had not been included in any phylogenetic analyses until this study, although differences in skull morphology from other *Tomistoma* species had been noted (Jouve *et al.*, 2015). Both CW3 and RW3 analyses resolve *T. dowsoni* as part of Gavialoidea, most closely related to *Piscogavialis*.

Crocodyloidea

In our CW3 and RW3 analyses, Crocodyloidea is composed of three clades: Tomistominae, Crocodylinae and an early diverging crocodyloid clade consisting of *Brachyuranochampsa*, *Crocodylus affinis* Marsh, 1871, *C. elliotti* Leidy, 1871, *C.* cf. *clavis* Cope, 1871 and *Prodiplocynodon* (Fig. 6). This latter clade is united by: foramen for the palatine ramus of CN-V large (at least 50% or more of adjacent alveolus length) (character 137); basisphenoid not exposed laterally on braincase (character 317); and anterior median palatine process into maxilla does not extend beyond anterior end of the suborbital fenestrae (character 370).

The relationships we identify in Tomistominae are similar to those found by Brochu (1999), Jouve *et al.* (2008b) and Buscalioni *et al.* (2011). However, unlike the topologies generated by Brochu (2004) and Jouve *et al.* (2015), three of the four *Tomistoma* species scored in our dataset (all except *T. dowsoni*) were resolved as the most deeply nested tomistomines in both CW3 and RW3 [Fig. 6; Supporting Information (S3)]. This includes *T. petrolica* Yeh, 1958, which had been placed in an earlier diverging position elsewhere (Brochu & Storrs, 2012); but not discussed). These tomistomines cluster together based on the following characters: a small pit posterior to the external nares (character 107); linear lateral margins of maxillae in dorsal view (character 127); a straight ventral edge of the maxillae in lateral view (character 128); anteriormost extension of the nasal located posterior relative to the level of the first maxillary tooth (character 152); absence of a parietopostorbital suture from the skull roof (character 244); and thin and long teeth, at least three times longer than wide (character 397).

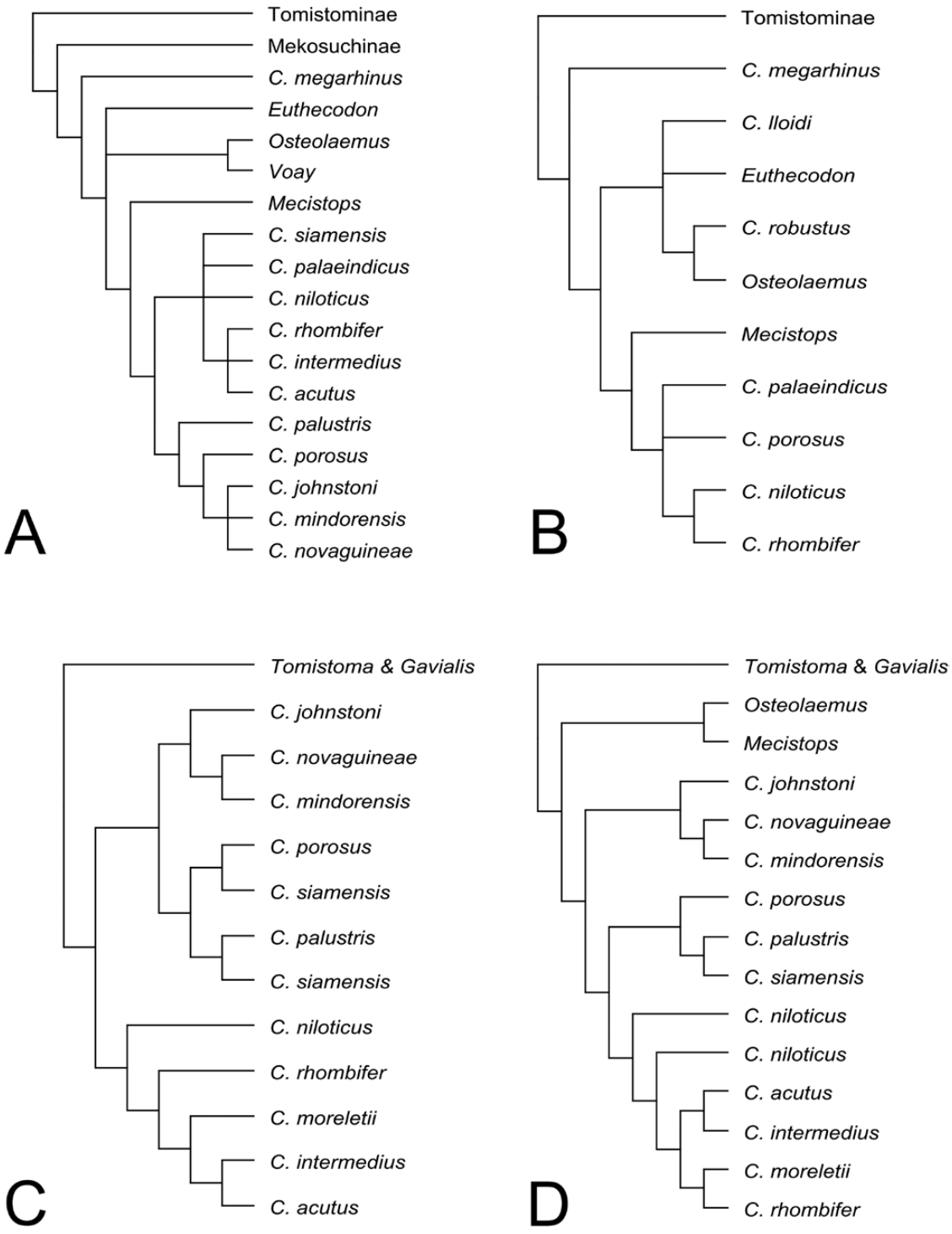

Figure 9. Summary of the competing hypotheses of crocodyloid phylogenetic relationships based on the following analyses: A, Brochu & Storrs (2012), morphological; B, Brochu (1999), morphological; C, Meredith *et al.* (2011), molecular, mitochondrial DNA; D, Oaks (2011), molecular, mitochondrial & nuclear DNA.

The interrelationships of Crocodylinae are highly variable across our different analyses. The topologies we found with our CW3 analysis differ from those published by others, on the basis of both morphological (Brochu & Storrs, 2012) and molecular (Meredith *et al.*, 2011; Oaks, 2011) (Fig. 9) datasets, and do not

cluster species geographically [e.g. into 'Old World' and 'New World' groups, as found by Meredith *et al.* (2011)]. These interrelationships are supported by few synapomorphies for the groups in Crocodylinae, but there are a high number of shifts within continuous characters. In this case, the reliance of continuous characters on overall skull shape appears to be a potential cause for the unique interrelationships found. In addition, most discrete characters that act as synapomorphies for the different clades of Crocodyinae are located in the posterior skull and/or mandible (e.g. features of the basicoccipital and dentary). However, many of these clades are based on continuous characters and are thus variable between analyses.

In addition, several 'traditional' non-crocodyline taxa, such as *C. depressifrons* de Blainville, 1855, *Asiatosuchus grangeri* Mook, 1940 (both crocodyloids according to: Delfino & Smith, 2009; Brochu & Storrs, 2012; Wang *et al.*, 2016) and *Eoalligator huiningensis* Young, 1982 (a crocodyloid according to: Wu *et al.*, 2018), are resolved as part of a monophyletic group nested deeply within Crocodylinae in both the CW3 and RW3 analyses. However, this group is united only by a single character state: a 'neck' formed by the pterygoid surface being pushed inward, lateral and anterior to the internal choana (character 357).

Alligatoroidea

Two of the largest deviations from 'traditional' crocodylian phylogenies seen in our trees occur in Alligatoroidea. The CW3 analysis resolves Diplocynodontinae as the sister-group to all Brevirostres, instead of placing it in Alligatoroidea (as in: Delfino & Smith, 2012; Brochu, 2013; and our RW3 trees, as well as the constrained CW3 trees). *Leidyosuchus gilmorei* + *Leidyosuchus canadensis* is placed as the sister-group of Diplocynodontinae in the CW3 analysis. This association is supported by the following characters: frontal preventing contact between postorbital and parietal on skull table (character 193); spina quadratojugalis positioned high between posterior and superior angles of infratemporal fenestra (character 270); and dentary alveoli 3 and 4 confluent (character 420). This is in contrast to the relationship proposed by Delfino & Smith (2012) where *Leidyosuchus* is placed as the sister-taxon of Diplocynodontinae + Globidonta (but not discussed in their paper). However, our results agree with Delfino & Smith (2012) in finding that *Baryphracta deponiae* is nested deeply within *Diplocynodon*.

We agree with Wu *et al.* (2018) that *Eoalligator* and *Asiatosuchus* are not synonymous (*contra* Wang *et al.*, 2016). Our findings corroborate the identification of *Asiatosuchus* as a crocodyloid (Delfino & Smith, 2009; Wang *et al.*, 2016) and also suggest a possible crocodyloid position for *Eoalligator huiningensis* (see above). However, *E. chunyii* is placed as the sister-taxon to Brevirostres in the CW3 analysis.

The largest differences between our results and those of previous analyses are found in the relationships within Globidonta. Although Caimaninae is resolved as monophyletic, Alligatorinae is paraphyletic in both the CW3 and RW3 analyses, in marked contrast to the analysis of Brochu (2013) and its derivatives (e.g. Skutschas *et al.*, 2014; Wang *et al.*, 2016) (Fig. 6). The overall relationships in Alligatorinae that are supported here resemble those in Wu *et al.* (1996), although that study did not include any caimanines. As with Crocodylinae, there are few discrete synapomorphies supporting the internal alligatorine groups in our trees: instead, there are a large number of shifts in continuous characters. Our results mainly reflect the patterns of overall skull shape within Alligatorinae (e.g. the shorter snouts of both *A. sinensis* Fauvel, 1879 and caimans), potentially because of the influence of continuous data, although Alligatorinae remains paraphyletic in the phylogenies based on the rediscretized datasets (RW3 and RW12).

Molecules vs. morphology

Our reconstructed morphological phylogenies differ from recently proposed molecular trees for extant crocodilian taxa in a number of ways. As outlined above, relationships differ most notably within the Crocodylinae, the paraphyly of Alligatorinae, as well as in providing a different topology for the well-known *Gavialis–Tomistoma* problem (see below). The results of molecular analyses, based on both nuclear and mitochondrial data, have usually been consistent between different studies and corresponded to biogeographical patterns (Oaks 2011). One possible explanation for the differences between the molecular and morphological trees lies in the use of continuous characters, as we have discussed previously. The relationships within the Crocodylinae and Alligatorinae are usually determined by shifts between continuous character states, which follow changes in the general outlines of the skull for the most part. In addition, a simple parsimony analysis of our dataset without EIW, and with continuous characters removed, yielded a large unresolved tree (data not shown). A second analysis of our dataset without continuous characters but with the use of EIW (k = 3) resulted in a similar topology to the CW3 tree, with a paraphyletic Alligatorinae and unique relationships within Crocodylinae. This indicates that the use of continuous characters does not constitute

the sole reason for the differences between molecular trees and our morphological phylogenies. Additional reasons for these differences could include: (1) EIW potentially penalizes the characters that underpin the relationships in the affected subfamilies and/or (2) errors caused in molecular phylogenetic topologies because they exclude fossil species.

Temporal implications

The temporal ranges implied by our phylogenies (Fig. 10) are influenced strongly by the differing positions of Hylaeochampsidae and *Crocodilaemus robustus* within our trees. The node ages obtained here are usually older than those derived from molecular phylogenetic estimates (e.g. Roos *et al.*, 2007; Oaks, 2011).

Our results indicate that the origin of Neosuchia occurred in the Early Jurassic, at least 180 million years ago (Mya), which is consistent with other estimates (Pol *et al.*, 2009; Montefeltro *et al.*, 2013). The origination time of Eusuchia is strongly influenced by the placement of *Crocodilaemus*: if the latter is the sister-taxon of Brevirostres, as in the tree based on the CW3 analysis, eusuchian origins are pushed back to the early Late Jurassic (around 160 Mya). However, if *Crocodilaemus* is removed, the CW3 tree places eusuchian origins in the early part of the Early Cretaceous, around 130 Mya (Fig. 10). The latter is similar to the timing implied by the constrained CW3 trees. This estimate is congruent with those from Pol *et al.* (2009) and Lee & Yates (2018). The placement of Hylaeochampsidae and *Crocodilaemus robustus* also adds long ghost ranges of ~70 Myr to Gavialoidea and the *Borealosuchus* clade in the unconstrained CW3 tree. In contrast, the differing placements of Diplocynodontinae do not affect the origination time of Crocodylia, which is estimated to have taken place ~90–100 Mya. This estimate agrees with the recent discovery of the earliest potential crocodylian, from the Cenomanian (Mateus *et al.*, 2018).

In agreement with Brochu (2003), Martin & Delfino (2010) and Brochu *et al.* (2012), all of the major crocodylian lineages (crocodyloids, including tomistomines, alligatoroids and gavialoids) appeared before the K/Pg boundary. In addition to the three extant lineages, the fossil record shows that

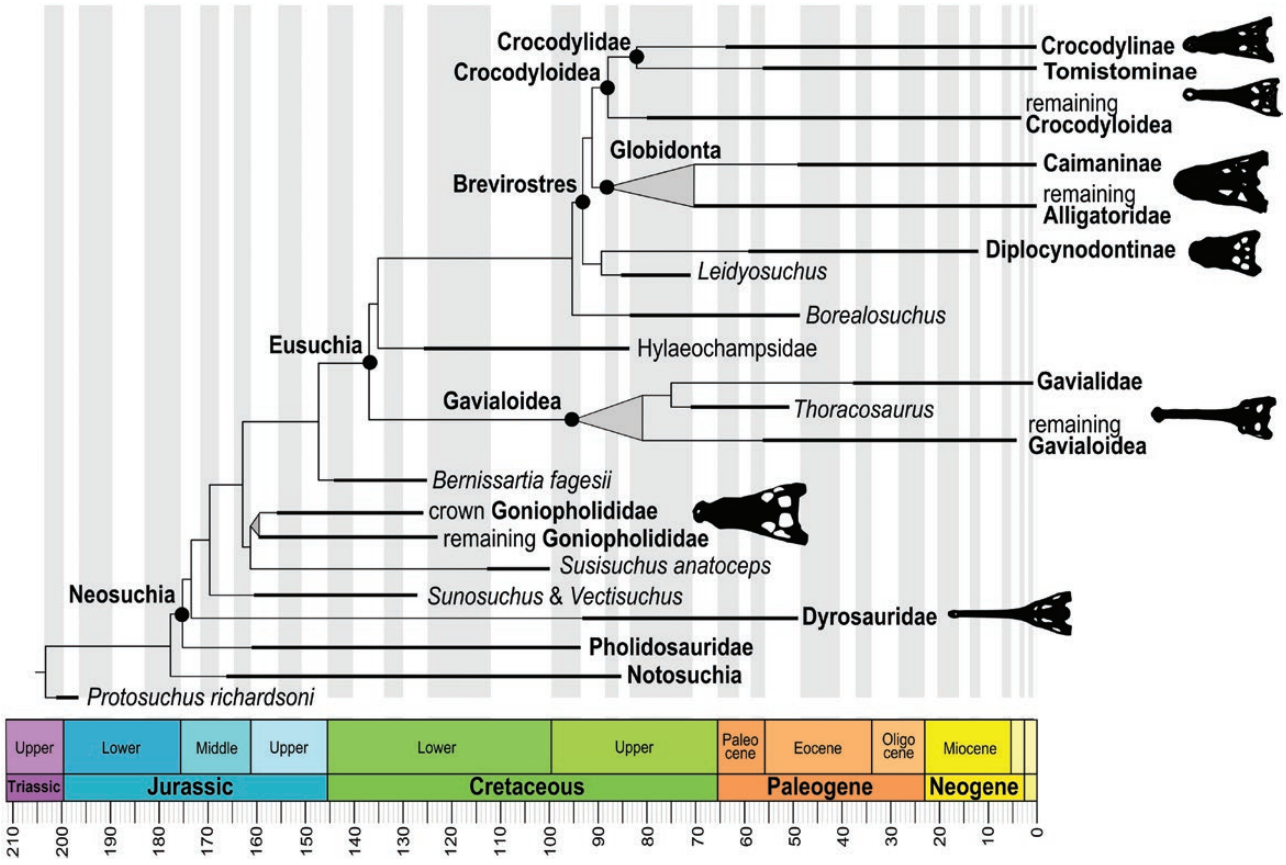

Figure 10. Summarized and timescaled strict consensus tree from the unconstrained CW3 analysis. Original image created with the R package *strap* (Bell & Lloyd, 2014). Image modifications and skull outline drawings by the lead author.

Tethysuchia and Sebecosuchia both survived the K/Pg boundary, as also noted by Pol & Larsson (2011) and reflected in our tree topologies.

The origin of Tomistominae is extended much further back in time by our analyses. Instead of appearing after the K/Pg boundary (e.g. Brochu, 2003; Salisbury *et al.*, 2006), our CW3 trees consistently place the split of this major group from the remaining Crocodylidae in the Late Cretaceous around 81 Mya or earlier (Fig. 10). This also adds a long (27 million years) ghost range to the base of the tomistomine lineage. The early split of tomistomines from the remaining crocodyloid lineage might be due to the placement of Hylaeochampsidae, which, in turn, pulls back the origination date for Brevirostres as a whole. In addition, many previous studies have based their origination estimates on the appearance dates of the first fossils in a group [such as Brochu (2003) and Salisbury *et al.* (2006)], rather than using statistical time-calibration methods, including ghost lineages, for calculating the timing of lineage splits.

Convergent evolution of longirostry and the assembly of the long and narrow snout

The longirostrine problem, and the probably inaccurate taxon clustering it creates in crocodylomorph phylogenies, has been recognized for several decades (Clark, 1994; Jouve, 2009; Meunier & Larsson, 2016). There have been previous studies of the functional morphology and convergence of longirostrine crocodylomorph snouts (e.g. Salas-Gismondi *et al.*, 2016; Ballell *et al.*, 2019). Furthermore, insights into the longirostrine condition have come from recent work on the embryological developmemt of extant crocodylian skulls by Morris *et al.* (2019). These authors found that heterochrony is responsible for the convergent trends in crocodylian snout evolution and that the longirostrine shape can be achieved by several different ontogenetic trajectories during development. However, to date, no previous analysis has examined in detail the character-state changes that occurred during the parallel assembly of elongate snouts in neosuchians.

Here, we find that the occurrence of rampant homoplasy in snout length is also supported by the stratigraphic distribution of longirostrine taxa. One of the most striking examples of the impact of longirostrine characters on phylogenetic topology is illustrated by the placement of Thalattosuchia. This group has been placed almost everywhere in the crocodylomorph tree, from nesting within Neosuchia (often in association with other longirostrine clades, such as members of Tethysuchia: Pol & Gasparini, 2009; Bronzati *et al.*, 2012) to a position outside Neosuchia (Benton & Clark, 1988; Sereno *et al.*, 2001; Wu *et al.*, 2001; Young & De Andrade, 2009; Holliday & Gardner, 2012). We observed similar patterns in our unweighted and Bayesian analyses, with Thalattosuchia clustering with other longirostrine clades (Fig. 4). However, Thalattosuchia is found to lie outside Neosuchia in all of our weighted analyses.

Our results are consistent with Brochu's (2001) proposal that long-snouted forms evolved on at least three occasions within Neosuchia: in Gavialoidea, Tomistominae and Tethysuchia. Additionally, longirostry evolved independently in at least three taxa within the otherwise short-snouted Crocodylinae: *Euthecodon arambourgi* Ginsburg & Buffetaut, 1978, *Mecistops cataphractus* Cuvier, 1825 and *Crocodylus johnstoni* (the latter was not examined first-hand and is, therefore, missing from our dataset). However, in contrast to Brochu (2001), the crocodyline taxon *Crocodylus intermedius* is not a truly longirostrine taxon as defined in the current study (see above). Molecular studies reduce the number of independent origins of the longirostrine condition by at least one, with Gavialoidea and Tomistominae usually forming a clade (Piras *et al.*, 2010; see below).

Character-state mapping on the strict consensus tree of the unconstrained CW3 analysis (Fig. 6) revealed that at least 24 characters are associated with the evolution of longirostrine clades (Fig. 11; see Table 4 for detailed character descriptions). Twelve of these characters appear to be linked to the evolution of longirostry in all three clades, as well as the three other independently occurring longirostrine species listed above. These features include skull and mandibular characters approximately equally. Preorbital ridges are lost at the base of all longirostrine clades and several others, such as Goniopholididae (character 87). The longirostrine snout is formed mainly from elongation of the premaxilla and maxilla, leading to straight ventral and lateral margins of the maxilla (characters 127 and 128). This is accompanied by the absence of raised alveolar walls relative to the ventral surface of the maxilla (character 131) and a change in the ventral structure of the premaxillary–maxillary contact, with a median projection of the premaxilla extending into the maxilla in the form of a sharp process (character 123). Furthermore, the maxillary teeth all remain the same size (character 386). There is less involvement from the nasal bones in snout elongation, because they loose contact with the external nares (character 149). Similar changes occur in the mandible: the shape of the dentary symphysis and involvement of the splenial in the symphysis play large roles. The splenial is usually involved extensively in the symphysis (characters 400 and 428), together with a relatively straight and long dentary (characters 401 and 402), leading to the characteristic 'Y'-shaped mandibular symphysis in all longirostrine taxa (character 468).

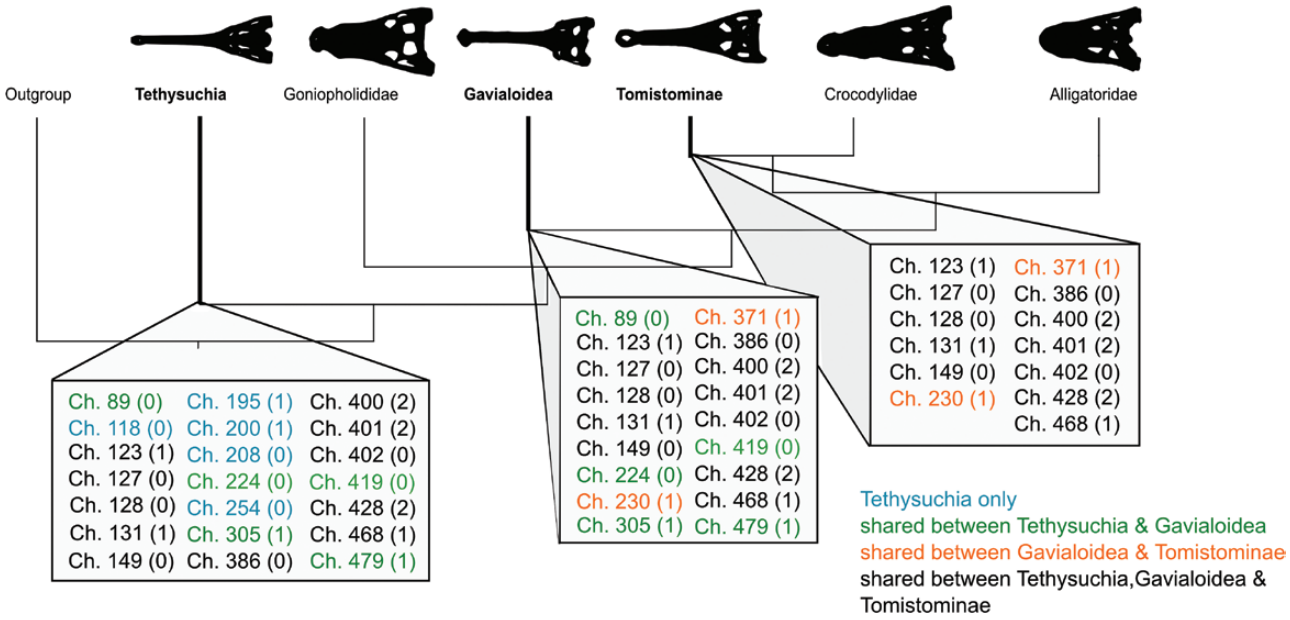

Figure 11. Characters associated with the evolution of the longirostrine condition mapped onto a simplified version of our neosuchian tree, based on analysis CW3. Note that character numbers do not denote synapomorphies for the clades; rather, these refer to characters that are shared by longirostrine clades. See Table 3 for detailed character state descriptions and positions. Outlines drawn by the lead author.

All of these changes occur independently at the base of each longirostrine clade. Although such 'sudden' and apparently coordinated state transformations might be an artefact generated by taxon sampling and specimen incompleteness, it is conceivable that these results point to a genuine, relatively rapid shift in snout morphology during a short time-interval, rather than a slower assembly of the longirostrine snout across several nodes.

In contrast to the anterior snout and mandible, far fewer posterior skull characters contribute to the independent derivation of the longirostrine condition in each of the long-snouted lineages (i.e. although some posterior skull character-states evolve at the base of longirostrine clades, they do not typically display the repeated coherent homoplasy seen in the more anterior portions of the snout and mandible). Tethysuchia, in particular, possesses several supratemporal region characters associated with its longirostrine condition (195 and 200) that are absent in other 'long-snouted' clades, indicating modification of the skull roof in these taxa as their snouts evolved. It is possible that these changes were related to the more marine lifestyles of many tethysuchians, which were almost unique to this clade within Neosuchia (Hill *et al.*, 2008). These features include the zigzag-shaped frontoparietal suture on the interfenestral bar (character 195), the anterolateral process of the postorbital (the presence of which is typical for Dyrosauridae) (character 200) and a complex skull roof surface (character 208). A complex skull roof surface is also found outside Neosuchia in Thalattosuchia, which contains many marine species (Wilberg, 2015b). In addition to the other skull roof changes, the placement of the postorbital is more anterior when compared to other neosuchians (character 254) and tethysuchians also share the absence of a ventral opening on the premaxilla-maxilla contact (character 118) with Alligatoridae.

Modifications of the posterior part of the skull also played some role in the evolution of gavialoid longirostry. Relatively large supratemporal fenestrae (character 224) and a ventrally sloping skull roof surface (character 89) are shared by gavialoids and tethysuchians. These changes are accompanied by bilateral tubera of the basioccipital (character 305), as well as a deep fork in the axial hypapophysis (character 479) in both Tethysuchia and Gavialoidea. The only anterior skull character that is uniquely shared by Gavialoidea and several tethysuchian taxa is the height of the alveolar wall of the fourth dentary tooth, which is level with that of the adjacent dentary alveoli (character 419). In addition, several posterior skull characters are unique to Gavialinae, such as an abrupt expansion of the orbits (character 88), a prominent notch at the ventral margin of the orbit (character 256) and a strongly arched posteroventral margin of the angular (character 442). However, The 'telescoping' and wide separation of the orbits has previously been revealed to be a potentially homoplastic feature in Gavialoidea (Salas-Gismondi *et al.*, 2016).

Table 4. Characters states revealed by character mapping to be common to one or more longirostrine clades with details of character state, character description and exact occurrence in the phylogenetic tree. Based on the strict consensus trees of the unconstrained CW3 analysis (Fig. 6)

Character number	Character state	Character description	Details of position
87	0	Preorbital ridges absent	Ancestral for all longirostrine clades, plus Alligatoroidea and Diplocynodontinae
123	1	Median projection of premaxilla at premaxillo–maxillary contact with sharp tips	In all longirostrine clades as well as *Euthecodon* and *Mecistops*
127	0	Lateral margins of snout linear, not festooned in dorsal view	In all longirostrine clades
128	0	Ventral edge of maxilla is straight in lateral view	In all longirostrine clades
131	1	Alveolar walls of maxillary level with ventral surface	In all Gavialoidea and Tomistominae, plus several Tethysuchia and goniopholidids
149	0	Nasal not in contact with external nares	In all longirostrine clades and Goniopholodidae
386	0	All maxillary teeth of similar size	in all longirostrine clades and *Euthecodon*
400	2	Extensions of symphysis beyond 8th alveolus	In all longirostrine clades
401	2	Anterior edge of symphysis transversally oriented, lateral edges longitudinal	In all longirostrine clades
402	0	Dorsal edge of dentary straight or slightly concave	In all longirostrine clades
428	2	Splenial involved extensively in symphysis	In all longirostrine clades
468	1	Mandible broadly 'Y'-shaped	In all longirostrine clades and Goniopholididae
118	0	No ventral opening on ventral edge of premaxillo-maxillary contact	In all Tethyschia and Alligatoridae
195	1	Frontoparietal suture on interfenestral bar zigzag in shape	In all Tethysuchia and *Tomistoma*
200	1	Well-developed anterolateral process on post-orbital	In all Tethysuchia
208	0	'Complex' supratemporal roof dorsal surface	In all Tethysuchia + Thalattosuchia
254	0	Postorbital bar placed anteriorly on jugal	In all Tethysuchia
89	0	Skull table surface slopes ventrally at maturity	In derived Gavialoidea and *Pholidosaurus* and *Dyrosaurus*
224	0	Supratemporal fenestrae large, covering more than 50% of skull roof	In all Tethysuchia and several gavialoids
305	1	Basioccipital with large bilateral pendulous tubera	In all Tethysuchia and Gavialoidea
419	0	4th dentary alveolus wall on level with adjacent dentary alveoli	In all Gavialoidea and *Sarcosuchus* and *Rhabdognathus*
479	1	Hypapophysis of axis with deep fork	In all scored Tethysuchia and Gavialoidea
230	1	Groove of external ear valve musculature flaring anteriorly	In all Gavialoidea and Tomistominae
371	1	Anterior median process of palatines into maxilla in form of thin wedge	In all Gavialoidea and Tomistominae
384	1	Flat depressions the size of small alveoli between maxillary and premaxillary alveoli	Only in *Gavialis*, *Mecistops*, *Rhabdognathus* and *Tomistoma*,
397	1	Thin and long teeth which are at least three times longer than wide	Ancestral state retained outside Eusuchia and in *Gavialis*, *Eogavialis* and *Tomistoma*

Gavialoids and tomistomines share two posterior skull characters that are potentially related to the formation of a long snout. The groove for the external ear valve musculature is flared anteriorly in both clades (character 230). Furthermore, the anterior process of the palatines into the maxilla takes the form of a thin wedge (character 371). There are two characters, 384 and 397, with shared character-states between *Gavialis* and *Tomistoma*, but that are absent in their direct ancestors (Table 4). This provides some evidence for their long-snoutedness as a homoplastic condition, in direct contrast to hypotheses derived from molecular evidence alone (Piras *et al.*, 2010).

Molecular studies have consistently grouped *Gavialis* and *Tomistoma* as sister-taxa, postulating a single origin of longirostry at least for extant forms (Roos *et al.*, 2007; Piras *et al.*, 2010; Oaks 2011). Recently, new fossil taxa have been described that exhibit both gavialine and tomistomine features, providing support for the molecular hypotheses (Iijima & Kobayashi, 2019). Our results conflict with these evolutionary hypotheses potentially for two reasons: (1) morphological data, in general, is potentially biased towards phylogenetic signals that override the characters connecting *Gavialis* and *Tomistoma* (Iijima & Kobayashi, 2019) and/or (2) the topology favoured by molecular or total evidence analyses is incorrect, because it fails to sufficiently sample fossil taxa near the bases of the tomistomine and gavial lineages that reinforce separate origins (see below).

The most important aspect of the longirostrine problem in both molecular and morphological analyses is taxon sampling: most analyses combining molecular and morphological evidence (e.g. Gold *et al.*, 2014; Iijima & Kobayashi, 2019) only investigated Crocodylia. However, if *Gavialis* and *Tomistoma* are constrained to be sister-taxa in accordance with molecular phylogenies, total evidence analyses including longirostrine groups outside Crocodylia (such as Tethysuchia) cluster all longirostrine taxa together (Groh *et al.*, unpublished material), regardless of their stratigraphic position. Future investigations of the '*Tomistoma–Gavialis* problem' should take these factors into account.

Overall, based on the results in this study, the evolution of the longirostrine condition seems to have been remarkably constrained, at least with regards to the anterior portion of the skull, and occurred in a broadly similar fashion in each of the different clades. Modifications to the premaxilla, maxilla, dentary and splenial were of primary importance in the convergent construction of the long-snouted condition. In contrast, the median parts of the skull and mandible between the anterior and posterior parts remained mostly unmodified, although changes involving the orbits can be related to different feeding mechanisms (e.g. in some gavialoid species: Salas-Gismondi *et al.*, 2016). Moreover, the posterior part of the skull evolved in a less constrained manner with separate adaptations present in each of the longirostrine clades. These unique posterior skull features potentially represent adaptations to different habitats and feeding styles. For example, it is notable that tethysuchians possess a much larger number of unique character states related to the acquisition of the long snout than the other 'longirostrine' clades. Furthermore, Tethysuchia and Gavialoidea exhibit more similarities in their snout assembly than Gavialoidea and Tomistominae (Table 4). Once again, this emphasizes the dissimilarities between the latter two groups. These results partially corroborate the findings of Morris *et al.* (2019), who observed that *Gavialis* and *Tomistoma* are the only exceptions to a pattern of otherwise conserved regions of morphospace during early and median skeletal development stages of extant crocodylian species. In addition, these authors found that a number of different developmental pathways could lead to similar snout morphologies, emphasizing the depth of convergence in crocodylian skull evolution, which is consistent with our conclusions here.

In order to test our results further, the genetic patterns underpinning longirostrine snout development should be investigated in both *Gavialis* and *Tomistoma*, which would provide new data that could potentially resolve the ongoing *Gavialis–Tomistoma* debate (Gatesy *et al.*, 2003; Piras *et al.*, 2010; Gold *et al.*, 2014).

CONCLUSIONS

In this case study we demonstrate that the combined application of continuous data and EIW can result in improved stratigraphic fit of phylogenetic trees, in spite of the presence of a strong homoplastic signal (at least compared to other vertebrate groups). Even though several studies confirm their utility (e.g. Parins-Fukuchi, 2017; Jones & Butler, 2018), the influence of continuous characters on large-scale phylogenetic studies is still largely unexplored, and future work should concentrate on determining the effects of continuous characters and EIW on more taxonomic datasets. Despite the large number of morphological characters used in this study, character quality is equally important,and this work highlights the need to construct characters more critically and to test them rigorously before including them in phylogenetic analyses.

Our new neosuchian phylogeny is generally consistent with those derived from previous analyses, confirming the placement of Tethysuchia at the base of Neosuchia. However, it deviates from established phylogenetic hypotheses in the identification of alligatorine paraphyly, the lack of resolution within

Crocodylinae, and in the uncertain positions of Diplocynodontinae and Hylaeochampsidae. In addition, the origin of Tomistominae is estimated to have occurred earlier than in most previous studies. Future datasets should aim to include additional members of clades that were either unrepresented or represented by only a single taxon in this phylogeny, such as Atoposauridae.

Character mapping reveals that the longirostrine condition was assembled in similar ways across the neosuchian tree by transformation of the anterior portions of the snout and mandible. However, posterior skull transformations are often unique to individual longirostrine clades and might represent adaptations to their different habitats and lifestyles. Future work should be aimed at investigating the genetic mechanisms that underlie long snout evolution and the particular ways in which evolution of longirostry might have occurred in different environments.

ACKNOWLEDGEMENTS

Financial support for this study was provided by the London NERC DTP (Ref NE/L002485/1) and the UCL Bogue Fellowship. The authors thank Lorna Steel and Susie Maidment (NHMUK), Patrick Campbell (NHMUK), Carl Mehling (AMNH), Michael Brett-Surman (USNM), Daniel Brinkman (YPM), Rainer Schoch (SMNS), Liu Jun (IVPP), Wolfgang Munk (SMNK), Ronan Allain (MNHN), Annelise Folie (IRScNB) and Dean Veall (LDUCZ) for their support and access to the specimens. Thanks also go to the Willi Hennig Society for its continuing support of the TNT phylogenetics package and Alexander N. Schmidt-Lebuhn and Martin Ramírez for the scripts used in our analyses. We also thank the referees (Roland Sookias and two anonymous reviewers) and Associate Editor for comments that helped improve this paper.

REFERENCES

Aberer AJ, **Krompass D**, **Stamatakis A. 2013.** Pruning rogue taxa improves phylogenetic accuracy: an efficient algorithm and webservice. *Systematic Biology* **62:** 162–166.

Adams TL, **2014.** Small crocodyliform from the Lower Cretaceous (Late Aptian) of central Texas and its systematic relationship to the evolution of Eusuchia. *Journal of Paleontology* **88:** 1031–1049.

Adams DC, **Felice RN. 2014.** Assessing trait covariation and morphological integration on phylogenies using evolutionary covariance matrices. *PLoS ONE* **9:** e94335.

Alroy J, **Carrano MT**, **Mannion PD**, **Behrensmeyer AK**, **Uhen MD. 2018.** Taxonomic occurrences of Crocodylomorpha recorded in fossilworks, the evolution of terrestrial ecosystems database, and the paleobiology database. *Fossilworks*. Available at: http://fossilworks.org (accessed 07 November 2018).

Ausich WI, **Kammer TW**, **Rhenberg EC**, **Wright DF. 2015.** Early phylogeny of crinoids within the pelmatozoan clade. *Palaeontology* **58:** 937–952.

Ballell A, **Moon BC**, **Porro LB**, **Benton MJ**, **Rayfield EJ. 2019.** Convergence and functional evolution of longirostry in crocodylomorphs. *Palaeontology* 1–21. doi: 10.1111/pala.12432.

Bell MA, **Lloyd GT 2014.** Strap: an R package for plotting phylogenies against stratigraphy and assessing their stratigraphic congruence. *Palaeontology* **58:** 1–11.

Benton MJ, **Clark JM. 1988.** Archosaur phylogeny and the relationships of the Crocodylia. In: Benton MJ, ed. *The phylogeny and classification of the tetrapods, volume 1*. New York: Oxford University Press, 295–338.

Benton MJ, **Storrs GW. 1994.** Testing the quality of the fossil record: paleontological knowledge is improving. *Geology* **22:** 111–114.

Bergsten J. 2005. A review of long-branch attraction. *Cladistics* **21:** 163–193.

Brazeau MD. 2011. Problematic character coding methods in morphology and their effects. *Biological Journal of the Linnean Society* **104:** 489–498.

Brochu CA. 1999. Phylogenetics, taxonomy, and historical biogeography of Alligatoroidea. *Journal of Vertebrate Paleontology* **19:** 9–100.

Brochu CA. 2001. Crocodylian snouts in space and time: phylogenetic approaches toward adaptive radiation. *American Zoologist* **41:** 564–585.

Brochu CA. 2003. Phylogenetic approaches toward crocodylian history. *Annual Review of Earth and Planetary Sciences* **31:** 357–397.

Brochu CA. 2004. A new Late Cretaceous gavialoid crocodylian from eastern North America and the phylogenetic relationships of thoracosaurs. *Journal of Vertebrate Paleontology* **24:** 610–633.

Brochu CA. 2007. Morphology, relationships, and biogeographical significance of an extinct horned crocodile (Crocodylia, Crocodylidae) from the Quaternary of Madagascar. *Zoological Journal of the Linnean Society* **150:** 835–863.

Brochu CA. 2011. Phylogenetic relationships of *Necrosuchus ionensis* Simpson, 1937 and the early history of caimanines. *Zoological Journal of the Linnean Society* **163:** 228–256.

Brochu CA. 2013. Phylogenetic relationships of Palaeogene ziphodont eusuchians and the status of *Pristichampsus* Gervais, 1853. *Earth and Environmental Science Transactions of The Royal Society of Edinburgh* **103:** 521–550.

Brochu CA, **Storrs GW. 2012.** A giant crocodile from the Plio-Pleistocene of Kenya, the phylogenetic relationships of Neogene African crocodylines, and the antiquity of *Crocodylus* in Africa. *Journal of Vertebrate Paleontology* **32:** 587–602.

Brochu CA, **Wagner JR**, **Jouve S**, **Sumrall CR**, **Densmore LD. 2009.** A correction corrected: consensus over the meaning of crocodylia and why it matters. *Systematic Biology* **58:** 537–543.

Brochu CA, **Parris DC**, **Grandstaff BS**, **Denton Jr RK**, **Gallagher WB. 2012.** A new species of *Borealosuchus* (Crocodyliformes, Eusuchia) from the Late Cretaceous–Early Paleogene of New Jersey. *Journal of Vertebrate Paleontology* **32:** 105–116.

Brocklehurst N, **Romano M**, **Fröbisch J. 2016.** Principal component analysis as an alternative treatment for morphometric characters: phylogeny of caseids as a case study. *Palaeontology* **59:** 877–886

Bronzati M, **Montefeltro FC**, **Langer MC. 2012.** A species-level supertree of Crocodyliformes. *Historical Biology* **24:** 598–606.

Buckland W. 1836. *Geology and mineralogy considered with reference to natural theology*, **Vol. 1**. London: G. Routledge & Company.

Buckley GA, **Brochu CA. 1999.** An enigmatic new crocodile from the Upper Cretaceous of Madagascar. *Special Papers in Palaeontology* **60:** 149–175.

Buckley GA, **Brochu CA**, **Krause DW**, **Pol D. 2000.** A pug-nosed crocodyliform from the Late Cretaceous of Madagascar. *Nature* **405:** 941–944.

Buscalioni AD, **Sanz JL. 1988.** Phylogenetic relationships of the Atoposauridae (Archosauria, Crocodylomorpha). *Historical Biology* **1:** 233–250.

Buscalioni AD, **Ortega F**, **Weishampel DB**, **Jianu CM. 2001.** A revision of the crocodyliform *Allodaposuchus precedens* from the Upper Cretaceous of the Hateg Basin, Romania. Its relevance in the phylogeny of Eusuchia. *Journal of Vertebrate Paleontology* **21:** 74–86.

Buscalioni AD, **Piras P**, **Vullo R**, **Signore M**, **Barbera C. 2011.** Early Eusuchia crocodylomorpha from the vertebrate-rich Plattenkalk of Pietraroia (Lower Albian, southern Apennines, Italy). *Zoological Journal of the Linnean Society* **163:** 199–S227.

Chamero B, **Buscalioni AD**, **Marugán-Lobón J**, **Sarris I. 2014.** 3D geometry and quantitative variation of the cervico-thoracic region in Crocodylia. *Anatomical record (Hoboken, N.J.: 2007)* **297:** 1278–1291.

Clark JM. 1994. Patterns of evolution in Mesozoic Crocodyliformes. In: Fraser NC, Sues HD, eds. *In the shadow of the dinosaurs: early Mesozoic tetrapods*. New York: Cambridge University Press, 84–97.

Clark JM, **Matthew J. 1986.** *Phylogenetic relationships of the crocodylomorph archosaurs*. Unpublished Doctoral Dissertation, University of Chicago.

Cohen KM, **Finney SC**, **Gibbard PL**, **Fan JX. 2013.** The ICS international chronostratigraphic chart. *Episodes* **36:** 199–204.

Congreve CR, **Lamsdell JC. 2016.** Implied weighting and its utility in palaeontological datasets: a study using modelled phylogenetic matrices. *Palaeontology* **59:** 447–462.

De Andrade RCLP, **Sayão JM. 2014.** Paleohistology and lifestyle inferences of a dyrosaurid (Archosauria: Crocodylomorpha) from Paraíba Basin (Northeastern Brazil). *PLoS ONE* **9:** e102189.

De Andrade MB, **Edmonds R**, **Benton MJ**, **Schouten R. 2011.** A new Berriasian species of *Goniopholis* (Mesoeucrocodylia, Neosuchia) from England, and a review of the genus. *Zoological Journal of the Linnean Society* **163:** 66–108.

Delfino M, **Smith T. 2009.** A reassessment of the morphology and taxonomic status of *"Crocodylus" depressifrons* (Crocodylia, Crocodyloidea) based on the early Eocene remains from Belgium. *Zoological Journal of the Linnean Society* **156:** 140–167.

Delfino M, **Smith T. 2012.** Reappraisal of the morphology and phylogenetic relationships of the middle Eocene alligatoroid *Diplocynodon deponiae* (Frey, Laemmert, and Riess, 1987) based on a three-dimensional specimen. *Journal of Vertebrate Paleontology* **32:** 1358–1369.

Farris JS. 1969. A successive approximations approach to character weighting. *Systematic Biology* **18:** 374–385.

Fortier DC, **Schultz CL. 2009.** A new neosuchian crocodylomorph (Crocodyliformes, Mesoeucrocodylia) from the Early Cretaceous of north-east Brazil. *Paleontology* **52:** 991–1007.

Fortier D, **Perea D**, **Schultz C. 2011.** Redescription and phylogenetic relationships of *Meridiosaurus vallisparadisi*, a pholidosaurid from the Late Jurassic of Uruguay. *Zoological Journal of the Linnean Society* **163:** 257–272.

Gasparini Z, **Chiappe LM**, **Fernandez M. 1991.** A new Senonian peirosaurid (Crocodylomorpha) from Argentina and a synopsis of the South American Cretaceous crocodilians. *Journal of Vertebrate Paleontology* **11:** 316–333.

Gasparini Z, **Pol D**, **Spalletti LA. 2006.** An unusual marine crocodyliform from the Jurassic-Cretaceous boundary of Patagonia. *Science* **311:** 70–73.

Gatesy J, **Springer MS. 2004.** A critique of matrix representation with parsimony supertrees. In: Bininda-Emonds ORP, ed. *Phylogenetic supertrees: combining information to reveal the tree of life*. Norwell: Kluwer Academic Publishers, 369–388.

Gatesy J, **Amato G**, **Norell M**, **DeSalle R**, **Hayashi C. 2003.** Combined support for wholesale taxic atavism in gavialine crocodylians. *Systematic Biology* **52:** 403–422.

Geiger DL, **Fitzhugh K**, **Thacker CE. 2001.** Timeless characters: a response to Vermeij (1999). *Paleobiology* **27:** 177–178.

Gold MEL, **Brochu CA**, **Norell MA. 2014.** An expanded combined evidence approach to the gavialis problem using geometric morphometric data from crocodylian braincases and eustachian systems. *PLoS ONE* **9:** e105793.

Goloboff PA. 1993. Estimating character weights during tree search. *Cladistics* **9:** 83–91.

Goloboff PA. 2014. Extended implied weighting. *Cladistics* **30:** 260–272.

Goloboff PA, **Catalano SA. 2016.** TNT version 1.5, including a full implementation of phylogenetic morphometrics. *Cladistics* **32:** 221–238.

Goloboff PA, **Szumik CA. 2015.** Identifying unstable taxa: efficient implementation of triplet-based measures of stability, and comparison with Phyutility and RogueNaRok. *Molecular Phylogenetics and Evolution* **88:** 93–104.

Goloboff PA, **Mattoni CI**, **Quinteros AS. 2006.** Continuous characters analyzed as such. *Cladistics* **22:** 589–601.

Goloboff PA, **Carpenter JM**, **Arias JS**, **Esquivel DRM. 2008.** Weighting against homoplasy improves phylogenetic analysis of morphological data sets. *Cladistics* **24:** 758–773.

Goloboff PA, **Torres A**, **Arias JS. 2017.** Weighted parsimony outperforms other methods of phylogenetic inference under models appropriate for morphology. *Cladistics* **34:** 407–437.

Gomani EM. 1997. A crocodyliform from the Early Cretaceous Dinosaur Beds, northern Malawi. *Journal of Vertebrate Paleontology* **17:** 280–294.

Grigg G, **Gans C. 1993.** Morphology and physiology of the Crocodylia. In: Glasby CG, Ross GJB, Beesley PL. *Fauna of Australia, Vol. 2A, Amphibia and Reptilia*. Canberra: Australian Government Publishing Service, 326–336.

Haeseler AV. 2012. Do we still need supertrees? *BMC Biology* **10:** 13.

Halliday TJ, **De Andrade MB**, **Benton MJ**, **Efimov MB. 2013.** A re-evaluation of goniopholidid crocodylomorph material from central asia: biogeographic and phylogenetic implications. *Acta Palaeontologica Polonica* **60:** 291–312.

Hastings AK, **Bloch JI**, **Cadena EA**, **Jaramillo CA. 2010.** A new small short-snouted dyrosaurid (Crocodylomorpha, Mesoeucrocodylia) from the Paleocene of northeastern Colombia. *Journal of Vertebrate Paleontology* **30:** 139–162.

Hastings AK, **Bloch JI**, **Jaramillo CA**, **Rincon AF**, **Macfadden BJ. 2013.** Systematics and biogeography of crocodylians from the Miocene of Panama. *Journal of Vertebrate Paleontology* **33:** 239–263.

Hekkala E, **Shirley MH**, **Amato G**, **Austin JD**, **Charter S**, **Thorbjarnarson J**, **Vliet KA**, **Houck ML**, **Desalle ROB**, **Blum MJ. 2011.** An ancient icon reveals new mysteries: mummy DNA resurrects a cryptic species within the Nile crocodile. *Molecular Ecology* **20:** 4199–4215.

Hill RV, **McCartney JA**, **Roberts E**, **Bouare M**, **Sissoko F**, **O'Leary MA. 2008.** Dyrosaurid (Crocodyliformes: Mesoeucrocodylia) fossils from the Upper Cretaceous and Paleogene of Mali: implications for phylogeny and survivorship across the K/T Boundary. *American Museum Novitates* **3631:** 1–20.

Holliday CM, **Gardner NM. 2012.** A new eusuchian crocodyliform with novel cranial integument and its significance for the origin and evolution of Crocodylia. *PLoS ONE* **7:** e30471.

Iijima M, **Kobayashi Y. 2019.** Mosaic nature in the skeleton of East Asian crocodylians fills the morphological gap between 'Tomistominae' and Gavialinae. *Cladistics*. doi: 10.1111/cla.12372

Iordansky NN. 1973. The skull of the Crocodilia. In: Gans C, Parsons TS. *Biology of the Reptilia*, **Vol. 4**. London and New York: Academic Press, 201–262.

Jones AS, **Butler RJ. 2018.** A new phylogenetic analysis of Phytosauria (Archosauria: Pseudosuchia) with the application of continuous and geometric morphometric character coding. *PeerJ* **6:** e5901.

Jouve S. 2009. The skull of *Teleosaurus cadomensis* (Crocodylomorpha; Thalattosuchia), and phylogenetic analysis of Thalattosuchia. *Journal of Vertebrate Paleontology* **29:** 88–102.

Jouve S, **Iarochene M**, **Bouya B**, **Amaghzaz M. 2005.** A new dyrosaurid crocodyliform from the Palaeocene of Morocco and a phylogenetic analysis of Dyrosauridae. *Acta Palaeontologica Polonica* **50:** 581–594.

Jouve S, **Iarochene M**, **Bouya B**, **Amaghzaz M. 2006.** A new species of *Dyrosaurus* (Crocodylomorpha, Dyrosauridae) from the early Eocene of Morocco: phylogenetic implications. *Zoological Journal of the Linnean Society* **148:** 603–656.

Jouve S, **Bouya B**, **Amaghzaz M. 2008a.** A long-snouted dyrosaurid (Crocodyliformes, Mesoeucrocodylia) from the Paleocene of Morocco: phylogenetic and palaeobiogeographic implications. *Palaeontology* **51:** 281–294.

Jouve S, **Bardet N**, **Jalil NE**, **Suberbiola XP**, **Bouya B**, **Amaghzaz M. 2008b.** The oldest African crocodylian: phylogeny, paleobiogeography, and differential survivorship of marine reptiles through the Cretaceous–Tertiary boundary. *Journal of Vertebrate Paleontology* **28:** 409–421.

Jouve S, **Bouya B**, **Amaghzaz M**, **Meslouh S. 2015.** *Maroccosuchus zennaroi* (Crocodylia: Tomistominae) from the Eocene of Morocco: phylogenetic and palaeobiogeographical implications of the basalmost tomistomine. *Journal of Systematic Palaeontology* **13:** 421–445.

Kluge AG, **Farris JS. 1969.** Quantitative phyletics and the evolution of anurans. *Systematic Biology* **18:** 1–32.

Koch NM, **Soto IM**, **Ramírez MJ. 2015.** Overcoming problems with the use of ratios as continuous characters for phylogenetic analyses. *Zoologica Scripta* **44:** 463–474.

Larsson H, **Gado B. 2000.** A new Early Cretaceous crocodyliform from Niger. *Neues Jahrbuch für Geologie und Paläontologie - Abhandlungen* **217:** 131–141.

Lauprasert K, **Cuny G**, **Thirakhupt K**, **Suteethorn V. 2009.** *Khoratosuchus jintasakuli* gen. et sp nov., an advanced neosuchian crocodyliform from the Early Cretaceous (Aptian–Albian) of NE Thailand. *Geological Society, London, Special Publications: Late Palaeozoic and Mesozoic Ecosystems in SE Asia* **315:** 175–187.

Lee MSY, **Yates AM. 2018.** Tip-dating and homoplasy: reconciling the shallow molecular divergences of modern gharials with their long fossil record. *Proceedings of the Royal Society B* **285:** 20181071.

Maddison WP. 1993. Missing data versus missing characters in phylogenetic analysis. *Systematic Biology* **42:** 576–581.

Maddison WP, **Maddison DR. 2017.** *Mesquite: a modular system for evolutionary analysis. Version 3.2*. Available at: http://mesquiteproject.org (accessed 01 November 2018).

Mannion PD, **Upchurch P**, **Barnes RN**, **Mateus O. 2013.** Osteology of the Late Jurassic Portuguese sauropod dinosaur *Lusotitan atalaiensis* (Macronaria) and the evolutionary history of basal titanosauriforms. *Zoological Journal of the Linnean Society* **168:** 98–206.

Mannion PD, **Benson RBJ**, **Carrano MT**, **Tennant JP**, **Judd J**, **Butler RJ. 2015.** Climate constrains the evolutionary history and biodiversity of crocodylians. *Nature Communications* **6:** 8438.

Martin JE, **Buffetaut E. 2008.** *Crocodilus affuvelensis* Matheron, 1869 from the Late Cretaceous of southern France: a reassessment. *Zoological Journal of the Linnean Society* **152:** 567–580.

Martin JE, **Delfino M. 2010.** Recent advances in the comprehension of the biogeography of Cretaceous European eusuchians. *Palaeogeography, Palaeoclimatology, Palaeoecology* **293:** 406–418.

Martin JE, **Rabi M**, **Csiki Z. 2010.** Survival of *Theriosuchus* (Mesoeucrocodylia: Atoposauridae) in a Late Cretaceous archipelago: a new species from the Maastrichtian of Romania. *Die Naturwissenschaften* **97:** 845–854.

Martin JE, **Smith T**, **Broin FDLD**, **Escuillié F**, **Delfino M. 2014.** Late Palaeocene eusuchian remains from Mont de Berru, France, and the origin of the alligatoroid *Diplocynodon*. *Zoological Journal of the Linnean Society* **172:** 867–891.

Martin JE, **Delfino M**, **Smith T. 2016a**. Osteology and affinities of Dollo's goniopholidid (Mesoeucrocodylia) from the Early Cretaceous of Bernissart, Belgium. *Journal of Vertebrate Paleontology* **36:** e1222534.

Martin JE, **Raslan-Loubatié J**, **Mazin JM. 2016b.** Cranial anatomy of *Pholidosaurus purbeckensis* from the Lower Cretaceous of France and its bearing on pholidosaurid affinities. *Cretaceous Research* **66:** 43–59.

Martinelli AG. 2003. New cranial remains of the bizarre notosuchid *Comahuesuchus brachybuccalis* (Archosauria, Crocodyliformes) from the Late Cretaceous of Rio Negro Province (Argentina). *Ameghiniana* **40:** 559–572.

Mateus O, **Puértolas-Pascual E**, **Callapez PM. 2018.** A new eusuchian crocodylomorph from the Cenomanian (Late Cretaceous) of Portugal reveals novel implications on the origin of Crocodylia. *Zoological Journal of the Linnean Society* **186:** 501–528.

Melstrom KM, **Irmis RB. 2019.** Repeated evolution of herbivorous crocodyliforms during the age of dinosaurs. *Current Biology* **29:** 2389–2395.

Meredith RW, **Hekkala ER**, **Amato G**, **Gatesy J. 2011.** A phylogenetic hypothesis for *Crocodylus* (Crocodylia) based on mitochondrial DNA: evidence for a trans-Atlantic voyage from Africa to the New World. *Molecular Phylogenetics and Evolution* **60:** 183–191.

Meunier LMV, **Larsson HCE. 2016.** Revision and phylogenetic affinities of *Elosuchus* (Crocodyliformes). *Zoological Journal of the Linnean Society* **179:** 169–200.

Meyer ER. 1984. Crocodilians as living fossils. In: Ginsburg RN, ed. *Living fossils, casebooks in earth sciences*. New York: Springer, 105–131.

Montefeltro FC, **Larsson HC**, **de França MA**, **Langer MC. 2013.** A new neosuchian with Asian affinities from the Jurassic of northeastern Brazil. *Die Naturwissenschaften* **100:** 835–841.

Morris ZS, **Vliet KA**, **Abzhanov A**,**Pierce SE. 2019.** Heterochronic shifts and conserved embryonic shape underlie crocodylian craniofacial disparity and convergence. *Proceedings of the Royal Society B* **286:** 20182389.

Norell MA, **Clark JM. 1990.** A reanalysis of *Bernissartia fagesii*, with comments on its phylogenetic position and its bearing on the origin and diagnosis of the Eusuchia. *Bulletin de l'Institut Royal des Sciences Naturelles de Belgique. Sciences de la Terre* **60:** 115–128.

Oaks JR. 2011. A time-calibrated species tree of Crocodylia reveals a recent radiation of the true crocodiles. *Evolution; international journal of organic evolution* **65:** 3285–3297.

O'Reilly JE, **Puttick MN**, **Parry L**, **Tanner AR**, **Tarver JE**, **Fleming J**, **Pisani D**, **Donoghue PCJ. 2016.** Bayesian methods outperform parsimony but at the expense of precision in the estimation of phylogeny from discrete morphological data. *Biology Letters* **12:** 20160081.

O'Reilly JE, **Puttick MN**, **Pisani D**, **Donoghue PCJ. 2018a.** Empirical realism of simulated data is more important than the model used to generate it: a reply to Goloboff *et al. Palaeontology* **61:** 631–635.

O'Reilly JE, **Puttick MN**, **Pisani D**, **Donoghue PCJ. 2018b.** Probabilistic methods surpass parsimony when assessing clade support in phylogenetic analyses of discrete morphological data. *Palaeontology* **61:** 105–118.

Ortega F, **Buscalioni AD**, **Gasparini Z. 1996.** Reinterpretation and new denomination of *Atacisaurus crassiproratus* (middle Eocene; Issel, France) as cf. *Iberosuchus* (Crocodylomorpha, Metasuchia). *Geobios* **29:** 353–364.

Ortega F, **Gasparini Z**, **Buscalioni AD**, **Calvo JO. 2000.** A new species of *Araripesuchus* (Crocodylomorpha, Mesoeucrocodylia) from the Lower Cretaceous of Patagonia (Argentina). *Journal of Vertebrate Paleontology* **20:** 57–76.

Ösi A, **Clark JM**, **Weishampel DB. 2007.** First report on a new basal eusuchian crocodyliform with multicusped teeth from the Upper Cretaceous (Santonian) of Hungary. *Neues Jahrbuch für Geologie und Paläontologie, Abhandlungen* **243:** 169–177.

Parins-Fukuchi C. 2017. Use of continuous traits can improve morphological phylogenetics. *Systematic Biology* **67:** 328–339.

Piras P, **Colangelo P**, **Adams DC**, **Buscalioni A**, **Cubo J**, **Kotsakis T**, **Meloro C**, **Raia P. 2010.** The *Gavialis–Tomistoma* debate: the contribution of skull ontogenetic allometry and growth trajectories to the study of crocodylian relationships. *Evolution & Development* **12:** 568–579.

Pol D. 2003. New remains of *Sphagesaurus huenei* (Crocodylomorpha: Mesoeucrocodylia) from the Late Cretaceous of Brazil. *Journal of Vertebrate Paleontology* **23:** 817–831.

Pol D, **Escapa IH. 2009.** Unstable taxa in cladistic analysis: identification and the assessment of relevant characters. *Cladistics* **25:** 515–527.

Pol D, **Gasparini Z. 2009.** Skull anatomy of *Dakosaurus andiniensis* (Thalattosuchia: Crocodylomorpha) and the phylogenetic position of Thalattosuchia. *Journal of Systematic Palaeontology* **7:** 163–197.

Pol D, **Larsson HCE. 2011.** First symposium on the evolution of crocodyliforms. *Zoological Journal of the Linnean Society* **163:** 1–6.

Pol D, **Norell MA. 2001.** Comments on the Manhattan Stratigraphic Measure. *Cladistics* **17:** 285–289.

Pol D, **Norell MA. 2004.** A new crocodyliform from Zos Canyon, Mongolia. *American Museum Novitates* **3445:** 1–36.

Pol D, **Norell MA**, **Siddall ME. 2004.** Measures of stratigraphic fit to phylogeny and their sensitivity to tree size, tree shape, and scale. *Cladistics* **20:** 64–75.

Pol D, **Turner AH**, **Norell MA. 2009.** Morphology of the Late Cretaceous crocodylomorph *Shamosuchus djadochtaensis* and a discussion of neosuchian phylogeny as related to the origin of Eusuchia. *Bulletin of the American Museum of Natural History* **324:** 1–103.

Puértolas E, **Canudo JI**, **Cruzado-Caballero P. 2011.** A new crocodylian from the late Maastrichtian of Spain: implications for the initial radiation of crocodyloids. *PLoS ONE* **6:** e20011.

Puttick MN, **O'Reilly JE**, **Tanner AR**, **Fleming JF**, **Clark J**, **Holloway L**, **Lozano-Fernandez J**, **Parry LA**, **Tarver JE**, **Pisani D**, **Donoghue PCJ. 2017.** Uncertain-tree: discriminating among competing approaches to the phylogenetic analysis of phenotype data. *Proceedings of the Royal Society B* **284:** 20162290.

R Core Team. **2016.** *R: a language and environment for statistical computing*. Vienna: R Foundation for Statistical Computing.

Randle E, **Sansom RS. 2017.** Phylogenetic relationships of the 'higher heterostracans' (Heterostraci: Pteraspidiformes and Cyathaspididae), extinct jawless vertebrates. *Zoological Journal of the Linnean Society* **181:** 910–926.

Rogers JV. 2003. *Pachycheilosuchus trinquei*, a new procoelous crocodyliform from the Lower Cretaceous (Albian) Glen Rose Formation of Texas. *Journal of Vertebrate Paleontology* **23:** 128–145.

Ronquist F, **Huelsenbeck JP. 2003.** MrBayes 3: Bayesian phylogenetic inference under mixed models. *Bioinformatics* **19:** 1572–1574.

Ronquist F, **Teslenko M**, **van der Mark P**, **Ayres DL**, **Darling A**, **Höhna S**, **Larget B**, **Liu L**, **Suchard MA**, **Huelsenbeck JP. 2012.** MrBayes 3.2: efficient Bayesian phylogenetic inference and model choice across a large model space. *Systematic Biology* **61:** 539–542.

Roos J, **Aggarwal RK**, **Janke A. 2007.** Extended mitogenomic phylogenetic analyses yield new insight into crocodylian evolution and their survival of the Cretaceous–Tertiary boundary. *Molecular Phylogenetics and Evolution* **45:** 663–673.

Salas-Gismondi R, **Flynn JJ**, **Baby P**, **Tejada-Lara JV**, **Claude J**, **Antoine PO. 2016.** A new 13 million year old gavialoid crocodylian from proto-Amazonian mega-wetlands reveals parallel evolutionary trends in skull shape linked to longirostry. *PloS ONE* **11:** e0152453.

Salisbury SW, **Molnar RE**, **Frey E**, **Willis PMA. 2006.** The origin of modern crocodyliforms: new evidence from the Cretaceous of Australia. *Proceedings of the Royal Society B* **273:** 2439–2448.

Sansom RS, **Choate PG**, **Keating JN**, **Randle E. 2018.** Parsimony, not Bayesian analysis, recovers more stratigraphically congruent phylogenetic trees. *Biology Letters* **14:** 20180263.

Schwarz-Wings D, **Klein N**, **Neumann C**, **Resch U. 2011.** A new partial skeleton of *Alligatorellus* (Crocodyliformes) associated with echinoids from the Late Jurassic (Tithonian) lithographic limestone of Kelheim, S-Germany. *Fossil Record* **14:** 195–205.

Seitz V, **Garcia S**, **Liston A. 2000.** Alternative coding strategies and the inapplicable data coding problem. *Taxon* **49:** 47–54.

Sereno PC. 2007. Logical basis for morphological characters in phylogenetics. *Cladistics* **23:** 565–587.

Sereno PC, **Larsson HCE. 2009.** Cretaceous crocodyliforms from the Sahara. *ZooKeys* **28:** 1–143.

Sereno PC, **Larsson HC**, **Sidor CA**, **Gado B. 2001.** The giant crocodyliform *Sarcosuchus* from the Cretaceous of Africa. *Science* **294:** 1516–1519.

Shirley MH, **Carr AN**, **Nestler JH**, **Vliet KA**, **Brochu CA. 2018.** Systematic revision of the living African Slender-snouted Crocodiles (*Mecistops* Gray, 1844). *Zootaxa* **4504:** 151–193.

Siddall ME. 1998. Stratigraphic fit to phylogenies: a proposed solution. *Cladistics* **14:** 201–208.

Skutschas PP, **Danilov IG**, **Kodrul TM**, **Jin J. 2014.** The first discovery of an alligatorid (Crocodylia, Alligatoroidea, Alligatoridae) in the Eocene of China. *Journal of Vertebrate Paleontology* **34:** 471–476.

Smith AB. 2000. Stratigraphy in phylogeny reconstruction. *Journal of Paleontology* **74:** 763–766.

Smith MR. 2019. Bayesian and parsimony approaches reconstruct informative trees from simulated morphological datasets. *Biology Letters* **15:** 20180632.

Stacklies W, **Redestig H**, **Scholz M**, **Walther D**, **Selbig J. 2007.** pcaMethods – a bioconductor package providing PCA methods for incomplete data. *Bioinformatics* **23:** 1164–1167.

Strong EE, **Lipscomb D. 1999.** Character coding and inapplicable data. *Cladistics* **15:** 363–371.

Sweetman SC, **Pedreira-Segade U**, **Vidovic SU. 2015.** A new bernissartiid crocodyliform from the Lower Cretaceous Wessex Formation (Wealden Group, Barremian) of the Isle of Wight, southern England. *Acta Palaeontologica Polonica* **60:** 257–268.

Templeton AR. 1983. Phylogenetic inference from restriction endonuclease cleavage site maps with particular reference to the evolution of humans and the Apes. *Evolution; International Journal of Organic Evolution* **37:** 221–244.

Tennant JP, **Mannion PD**, **Upchurch P. 2016.** Evolutionary relationships and systematics of Atoposauridae (Crocodylomorpha: Neosuchia): implications for the rise of Eusuchia. *Zoological Journal of the Linnean Society* **177:** 854–936.

Turner AH. 2004. Crocodyliform biogeography during the Cretaceous: evidence of Gondwanan vicariance from biogeographical analysis. *Proceedings of the Royal Societ B* **271:** 2003–2009.

Turner AH. 2015. A review of *Shamosuchus* and *Paralligator* (Crocodyliformes, Neosuchia) from the Cretaceous of Asia. *PLoS ONE* **10:** e0118116.

Turner AH, **Pritchard AC. 2015.** The monophyly of Susisuchidae (Crocodyliformes) and its phylogenetic placement in Neosuchia. *PeerJ* **3:** e759.

Tykoski RS, **Rowe TB**, **Ketcham RA**, **Colbert MW. 2002.** *Calsoyasuchus valliceps*, a new crocodyliform from the Early Jurassic Kayenta formation of Arizona. *Journal of Vertebrate Paleontology* **22:** 593–611.

Uyeda JC, **Caetano DS**, **Pennell MW. 2015.** Comparative analysis of principal components can be misleading. *Systematic Biology* **64:** 677–689.

Vogt L. 2018. The logical basis for coding ontologically dependent characters. *Cladistics* **34:** 438–458.

Wang YY, **Sullivan C**, **Liu J. 2016.** Taxonomic revision of *Eoalligator* (Crocodylia, Brevirostres) and the

paleogeographic origins of the Chinese alligatoroids. *PeerJ* **4:** e2356.

Wiens JJ. 2001. Character analysis in morphological phylogenetics: problems and solutions. *Systematic Biology* **50:** 689–699.

Wilberg EW. 2015a. What's in an outgroup? The impact of outgroup choice on the phylogenetic position of Thalattosuchia (Crocodylomorpha) and the origin of Crocodyliformes. *Systematic Biology* **64:** 621–637.

Wilberg EW. 2015b. A new metriorhynchoid (Crocodylomorpha, Thalattosuchia) from the Middle Jurassic of Oregon and the evolutionary timing of marine adaptations in thalattosuchian crocodylomorphs. *Journal of Vertebrate Paleontology* **35:** e902846.

Wilkinson M. 1995. A comparison of two methods of character construction. *Cladistics* **11:** 297–308.

Wills MA. 1999. Congruence between phylogeny and stratigraphy: randomization tests and the gap excess ratio. *Systematic Biology* **48:** 559–580.

Wold H. 1966. Estimation of principal components and related models by iterative least squares. In: Krishnaiah PP, ed. *Multivariate analysis*. New York: Academic Press, 391–420.

Wright AM, Hillis DM. 2014. Bayesian analysis using a simple likelihood model outperforms parsimony for estimation of phylogeny from discrete morphological data. *PLoS ONE* **9:** e109210.

Wu XC, Brinkman DB, Lu JC. 1994. A new species of *Shantungosuchus* from the Lower Cretaceous of Inner Mongolia (China), with comments on *S. chuhsienensis* Young, 1961 and the phylogenetic position of the genus. *Journal of Vertebrate Paleontology* **14:** 210–229.

Wu XC, Brinkman DB, Russell AP. 1996. A new alligator from the upper Cretaceaous of Canada and the relationship of early eusuchians. *Palaeontology* **39:** 351–376.

Wu XC, Sues HD, Dong ZM. 1997. *Sichuanosuchus shuhanensis*, a new Early Cretaceous protosuchian (Archosauria: Crocodyliformes) from Sichuan (China), and the monophyly of Protosuchia. *Journal of Vertebrate Paleontology* **17:** 89–103.

Wu XC, Russell AP, Cumbaa SL. 2001. *Terminonaris* (Archosauria: Crocodyliformes): new material from Saskatchewan, Canada, and comments on its phylogenetic relationships. *Journal of Vertebrate Paleontology* **21:** 492–514.

Wu XC, Li C, Wang YY. 2018. Taxonomic reassessment and phylogenetic test of *Asiatosuchus nanlingensis* Young, 1964 and *Eoalligator chunyii* Young, 1964. *Vertebrata PalAsiatica* **56:** 137–146.

Yang Z, Zhu T. 2018. Bayesian selection of misspecified models is overconfident and may cause spurious posterior probabilities for phylogenetic trees. *Proceedings of the National Academy of Sciences of the United Sates of America* **115:** 1854–1859.

Young MT, De Andrade MB. 2009. What is *Geosaurus*? Redescription of *Geosaurus giganteus* (Thalattosuchia: Metriorhynchidae) from the Upper Jurassic of Bayern, Germany. *Zoological Journal of the Linnean Society* **157:** 551–585.

Young MT, Bell MA, De Andrade MB, Brusatte SL. 2011. Body size estimation and evolution in metriorhynchid crocodylomorphs: implications for species diversification and niche partitioning. *Zoological Journal of the Linnean Society* **163:** 1199–1216.

Young MT, Steel L, Foffa D, Price T, Naish D, Tennant JP. 2014. Marine tethysuchian crocodyliform from the Aptian-Albian (Lower Cretaceous) of the Isle of Wight, UK. *Biological Journal of the Linnean Society* **113:** 854–871.

Young MT, Hastings AK, Allain R, Smith TJ. 2016. Revision of the enigmatic crocodyliform *Elosuchus felixi* de Lapparent de Broin, 2002 from the Lower-Upper Cretaceous boundary of Niger: potential evidence for an early origin of the clade Dyrosauridae. *Zoological Journal of the Linnean Society* **179:** 377–403.

SUPPORTING INFORMATION

Additional Supporting Information may be found in the online version of this article at the publisher's web-site.

Document S1. Full osteological character list with illustrations.
Document S2. List of rejected osteological characters from previous publications and the reasons for rejection.
Document S3. Strict consensus trees presented for all analyses.
Document S4. All .tnt files used for analysis and the tree file with the corresponding ages of the examined species used in strap.

APPENDIX

LIST OF SYNAPOMORPHIES

Synapomorphies are given for discrete characters and were obtained by using the 'List Synapomorphies' function in TNT v.1.5. Character numbers refer to the original character list of 569 characters [see Supporting Information (S1)]. Synapomorphies are listed for the tree in Figure 5, using the unconstrained analysis of CW3. For clade labels and phylogenetic definitions, see Figure 5. Character consistency indices (obtained with CharStats.run) are given after each character.

Notosuchia: Premaxillae loosely sutured anterior to nares (C92.1, CI = 1.00); anterior rostral contour concealed relative to external nares (C96.0, CI = 0.3);

perinarial fossa on premaxillae present (C102.1, CI = 1.00); no constriction of snout at maxilla-premaxilla contact (C113.0, CI = 0.1); two parallel ridges creating recess on lateral wall of premaxillary notch (C116.1, CI = 0.5); large and aligned neurovascular foramina on lateral surface of maxillae (C13.1, CI = 0.5); antorbital fenestra (C159.1, CI = 0.5); descending ornamented process at posterolateral edge of squamosal (C235.1, CI = 1.0); lateral surface of jugal exposed lateral to maxilla in ventral view (C258.0, CI = 0.3); major axis of quadrate ventrally directed (C273.1, CI = 1.0); subquadrangular morphology of distal end of quadrate in cross section (C280.1, CI = 1.0); quadrate with two distinct faces in posterior view (C281.1, CI = 1.0); dorsal margin of paroccipital process anterior to quadrate condyle (C289.1, CI = 0.1); paroccipital process curves downwards strongly in occipital view (C290.3, CI = 0.2); unsculpted region below dentary toothrow (C403.1, CI = 0.5); supraacetabular crest on ilium (C526.0, CI = 0.3); no articular anterior process on dorsal parasagittal osteoderms (C551.0, CI = 0.2); centra of vertebrae cylindrical in shape (C567.0, CI = 0.5).

Dyrosauridae: Maxillae project posterior to the level of postorbital bar (C141.1, CI = 0.3); postorbital bar slightly anterodorsally inclined (20° or less) (C211.1, CI = 0.3).

Pholidosauridae: Ventral edge of premaxilla is deeper than ventral edge of maxilla in lateral view (C112.1, CI = 0.3); zigzag shaped frontoparietal suture on interfenestral bar (C195.1, CI = 0.2); well-developed anterolateral process of the postorbital (C200.1, CI = 0.5).

Goniopholididae excl. Susisuchus: Depression on posterolateral surface of maxilla (C134.1, CI = 0.5).

'Deeply nested' Goniopholididae (Goniopholis, Amphicotylus, Anteophthalmosuchus): Crest dorsal to orbit on prefrontal-lacrimal (C168.1, CI = 0.1); quadratojugal forms posterior angle of infratemporal fenestra (C265.0, CI = 0.09).

Hylaeochampsidae: Posterior process on dorsal surface of maxilla (C144.1, CI = 0.07); no contact between lacrimal and nasal at medial edge (C160.0, CI = 0.1); lateral extension of lacrimal almost reaching the medial border of the orbit edge (C163.1, CI = 1.0); jugal does not exceed the anterior margin of orbit (C253.0, CI = 0.1); prominent and dorsally directed boss on the posterior surface of paroccipital process (C298.0, CI = 0.5); paroccipital process lateral to cranioquadrate opening barely extended posteriorly in dorsal view (C299.0, CI = 0.5).

Borealosuchus: Anterior median palatine process into maxilla in form of thin wedge (C371.1, CI = 0.1); dentary alveoli 3 and 4 confluent (C420.0, CI = 0.3); splenial reaches fifth dentary tooth (C427.0, CI = 0.1); lingual foramen on surangular-articular suture (C443.1, CI = 0.1).

Crocodylia incl. Hylaeochampsidae: Frontoparietal suture on skull table entirely (C193.2, CI = 0.1); parietopostorbital suture present within supratemporal fossa (C245.1, CI = 1.0); otic aperture closed posteriorly and of triangular shape, with dorsally directed apex (C323.1, CI = 0.5); palatines do not participate in anterior margin of choanae (C355.0, CI = 0.2); angular extends beyond posterior margin of orbits in lateral view (438.1, CI = 0.2); hypapophyseal keel present until eleventh cervical vertebra behind atlas (C483.1, CI = 0.3); all cervical vertebrae procoelous (C490.2, CI = 0.7); all thoracic vertebrae procoelous (C492.1, CI = 1.0); postacetabular process on ilium directed posteriorly (C530.1, CI = 1.0); osteoderm edges sutured to one another (C544.1, CI = 0.5).

Gavialoidea incl. Maroccosuchus: Frontoparietal suture entirely on skull table (C193.2, CI = 0.1); posterior walls of supratemporal fenestrae barely visible in dorsal view (C225.0, CI = 0.6); dorsal and ventral rims of groove for external ear valve musculature flaring anteriorly (C230.1, CI = 0.5); parietopostorbital suture present on dorsal skull roof (C244.1, CI = 0.09); no midline crest on basioccipital plate below occipital condyle (C304.0, CI = 0.07); basioccipital with large pendulous tubera (C305.1, CI = 0.1); dentary symphysis extends beyond eighth dentary alveolus (C400.2, CI = 0.1); lateral edges of dentary oriented longitudinally, with convex anterolateral corner and extensive transversely oriented anterior edge (C401.2, CI = 0.3); distal rami of mandible strongly curved medially at mid-length, giving the mandible a broad 'Y'-shape (C468.1, CI = 0.3).

Gavialinae: Ventral opening on ventral edge of premaxillo-maxillary contact (C118.1, CI = 0.06); transversely flattened postorbital bar (C210.0, CI = 0.06); prominent notch in ventral margin of orbits (C256.1,CI = 1.0); thin and long teeth, which are at least three times longer than wide (C397.1, CI = 0.2).

Brevirostres + Diplocynodontinae: Humeral shaft sigmoidal, with a pronounced posterior curvature of shaft on proximal area of humerus (C515.1,CI = 0.5).

Brevirostres (Crocodyloidea + Alligatoroidea): Dentary symphysis extends to sixth through eighth alveolus (C400.1, CI = 0.1); dorsal midline osteoderms rectangular (C548.1, CI = 0.7); more than one keel on presacral dorsal osteoderms (C556.1, CI = 1.0).

Crocodyloidea: Squamosal and quadrate extend dorsally along posterior margin of external auditory

meatus (C238.0, CI = 0.2); sulcus on anterior braincase wall lateral to basisphenoid rostrum (C315.1, CI = 0.5); interalveolar space between second and third dentary alveoli greater than that between first and second dentary alveoli (C417.1, CI = 0.1); anterior perforation on mandibular ramus of cranial nerve V on splenial absent (C431.1, CI = 0.1); one side of dorsal anterior forked process of surangular into dentary shorter than the other (C445.0, CI = 0.3); anterior margins of tuberculum and capitulum of sacral vertebrae nearly in same plane (C499.1, CI = 1.0); dorsal margin of iliac blade rounded with modest dorsal indentation (C522.1, CI = 0.3); follicle gland pores on ventral osteoderms absent (C560.1, CI = 1.0).

Crocodylidae: No posterior wall on median Eustachian foramen on basisphenoid (C318.1, CI = 0.3); lateral edges of palatines in anterior half of interfenestral bar parallel to subparallel (C366.0, CI = 0.07).

Tomistominae: Premaxillary ventral projections with sharp tips (C123.1, CI = 0.2); dorsal and ventral rims of groove for external ear valve musculature flaring anteriorly (C230.1, CI = 0.5); anterior suborbital fenestra extension posterior to anterior two-thirds of alveoli (C372.0, CI = 0.08); all dentary alveoli immediately posterior to fourth of similar size (C424.3, CI = 0.2); extensive involvement of splenial in mandibular symphysis (C428.2, CI = 0.2).

Crocodylinae: No extension of quadratojugal to superior angle of infratemporal fenestra (C267.0, CI = 0.2); otoccipitals participate in basioccipital tubera (C301.1, CI = 0.08).

Diplocynodontinae incl. Leidyosuchus: Frontal prevents contact between postorbital and parietal on skull table (C193.0, CI = 0.1); spina quadratojugalis positioned high between posterior and superior angles of infratemporal fenestra (C270.1, CI = 0.3); dentary alveoli 3 and 4 confluent (C420.0, CI = 0.3).

Diplocynodontinae excl. Leidyosuchus: Preorbital ridges reduced (C87.1, CI = 0.1); parietal and squamosal approach each other on posterior wall of supratemporal fenestra without making contact (C218.1, CI = 0.3); temporal canal hidden in dorsal view and overlapped by rim of supratemporal fossa (C226.1, CI = 0.08); lingual foramen for articular artery and alveolar nerve on surangular–articular suture (C443.1, CI = 0.2); posterior tip of iliac blade deep, less than twice as long as it is high (C523.1, CI = 1.0).

Alligatoridae: Premaxillae form less than ventral half of internarial bar (C101.1, CI = 0.2); no constriction of snout at premaxillo–maxillary contact (C113.0, CI = 0.1); no opening on ventral edge of premaxillo–maxillary contact (C118.0, CI = 0.06); maxillary alveoli heterodont (C390.1, CI = 0.1).

Caimaninae: Dorsal contour of rostrum concave in lateral view (C86.2, CI = 0.1); external nares confluent (C97.1, CI = 0.2); contact of lacrimals with nasal at medial edge (C160.1, CI = 0.1); no transverse ridge of frontals (C191.0, CI = 0.2); rim of supertemporal fenestrae overhangs fenestrae (C222.1, CI = 0.3); quadratojugal does not extend to superior angle of infratemporal fenestra (C267.0, CI = 0.2); dorsal exposure of supraoccipital (C286.1, CI = 0.07); dorsal margin of supraoccipital same height as dorsal margin of squamosal (C288.1, CI = 0.1); occipitals participate in basioccipital tubera (C301.1, CI = 0.08); ectopterygoid–pterygoid flexure remains throughout ontogeny (C332.1, CI = 1.0); last premaxillary tooth anterior to first maxillary tooth (C382.0, CI = 0.1); no anterior perforation on splenial for cranial nerve V (C431.1, CI = 0.1); angular does not extend beyond anterior end of foramen intermandibularis caudalis (C435.1, CI = 1.0); angular–surangular suture passes broadly along ventral margin of external mandibular fenestra (C441.1, CI = 0.1); contact of surangular–angular suture with articular dorsal to ventral tip (C448.1, CI = 1.0); surangular extends to posterior end of retroarticular process (C450.0, CI = 0.1); ventral process of coronoid remains largely on medial surface of mandible (C464.1, CI = 1.0); thin medial laminae at anterior end of atlantal ribs (C474.1, CI = 1.0); six nuchal osteoderms (C547.1, CI = 0.3); four contiguous dorsal osteoderms per row at maturity (C549.0, CI = 0.5); paired ossifications suturing osteoderms of ventral armour together (C562.1, CI = 0.3).

LIST OF EXAMINED SPECIMENS

†: extinct species

Alligator mcgrewi†: AMNH FR 8700, AMNH FR 7905

Alligator mefferdi†: AMNH FR 7016

Alligator mississippiensis: NHMUK X.184, NHMUK 1868.2.12.6, NHMUK 1873.2.21.2

Alligator prenasalis†: YPM VP 014063, YPM VP 026273

Alligator sinensis: IVPP V1335

Allognathosuchus heterodon†: AMNH FR 5157, FR 2088, FR 1257, USNM 16832, USNM 2508, USNM 13680, USNM 16835

Allognathosuchus mooki†: AMNH FR 6780

Allognathosuchus wartheni†: YPM VP 016989

Amphicotylus lucasii†: AMNH FR 5782 (as *Goniopholis lucasii*)
Anteophthalmosuchus hooleyi†: NHMUK PV R3876
Arambourgia gaudryi†: MNHN QU17155
Araripesuchus gomesii†: AMNH FR 24450
Asiatosuchus grangeri†: AMNH FR 6606, AMNH FR 6607, AMNH FR 6608
Asiatosuchus nanlingensis†: IVPP V 2772, IVPP V 2773
Bernissartia fagesii†: IRSNB 1538, NHMUK PV OR37712
Borealosuchus formidabilis†: YPM VP 016512 (as *Leidyosuchus formidabilis*)
Borealosuchus wilsoni†: AMNH FR 7637 (as *Leidyosuchus wilsoni*), USNM 12990
Boverisuchus vorax†: AMNH FR 29993 (as *Pristichampsa vorax*), USNM 12957 (as *Pristichampsus rollinatii*)
Brachychampsa montana†: AMNH FR 5032, USNM 7068
Brachyuranochampsa zangerli†: AMNH FR 6048, AMNH FR 16609, YPM VP 000246
Brochuchus pigotti†: NHMUK PV R7729
Caiman crocodilus: NHMUK 1946.4.463, NHMUK 1898.9.26.1, NHMUK 1846.4.21.10
Caiman latirostris: NHMUK 2009.1, NHMUK 1886.10.4.2, NHMUK 2008.270
Comahuesuchus brachybuccalis†: NHMUK PV R14104 (cast)
Congosaurus compressus†: MNHN TGE 4034, MNHN TGE 4036, MNHN TGE 4198
Crocodilaemus robustus†: USNM 15828, USNM 537820
Crocodylus acutus: NHMUK 1975.997
Crocodylus affinis†: USNM 18390, YPM VP 001345
Crocodylus clavis†: AMNH FR 1212, USNM 12719
Crocodylus depressifrons†: MNHN G 160
Crocodylus elliotti†: USNM 141, USNM 923, YPM VP 010075
Crocodylus intermedius: NHMUK 1851.8.25.29, NHMUK 1862.10.19.1
Crocodylus megarhinus†: AMNH FR 5061, AMNH FR 5095, YPM VP 058532, NHMUK PV R3327
Crocodylus moreletii: NHMUK 1861.4.1.4
Crocodylus niloticus: NHMUK 1967.1076, NHMUK 1934.6.3.1, NHMUK 1897.6.24.1
Crocodylus novaeguineae: NHMUK 1886.5.20.1, NHMUK 1886.5.20.2
Crocodylus palustris: NHMUK 1897.12.31.1 (as *Crocodylus palustris kimbula*), NHMUK 1848.2.5.9, NHMUK 1861.4.1.5
Crocodylus porosus: NHMUK 1847.3.5.33, NHMUK 1969.1590, NHMUK 1857.4.2.187
Crocodylus rhombifer: AMNH FR 16623, AMNH FR 16638, AMNH FR 6178, AMNH FR 6179
Crocodylus siamensis: NHMUK 1921.4.1.17, NHMUK 1921.4.1.168, NHMUK 1920.1.1626
Crocodylus silvalensis†: AMNH FR 1915, NHMUK PV OR39705
Diplocynodon hantoniensis†: AMNH FR 27632 (cast), NHMUK PV OR30393
Diplocynodon remensis†: IRSNB R289, MNHN F BR 4020, MNHN MB 051, MNHN BR 2622, MNHN BR 10085, MNHN BR 15976, MNHN BR 15200, MNHN BR 1645, MNHN BR 13106, MNHN BR 2617, MNHN BR 4021, MNHN BR 3171, MNHN BR 15197, MNHN BR 15227, MNHN BR 3649, MNHN BR 3636, MNHN BR 4244, MNHN BR 13695, MNHN BR 3663, MNHN BR 3634, MNHN BR 13418, MNHN BR 3639, MNHN BR 3631
Diplocynodon ungeri†: SMNK (unnumbered skull) (as *Diplocynodon steineri*)
Dollosuchoides densmorei†: IRSNB 1748
Dyrosaurus phosphaticus†: MNHN 1901–11, MNHN APH 27, MNHN APH 25, MNHN APH 23, MNHN unnumbered skull
Elosuchus cherifiensis†: MNHN MRS 340, MNHN SAM 129
Elosuchus felixi†: MNHN INA 21 (may be *Fortignathus*), MNHN INA 25, MNHN INA 3
Eoalligator chunyii†: IVPP V2716
Eoalligator huiningensis†: IVPP V4058
Eocaiman cavernensis†: AMNH FR 3158
Eogavialis africanum†: SMNS 11785
Eogavialis gavialoides†: AMNH FR 5066, AMNH FR 5067, AMNH FR 5069 (as *Gavialis gavialoides*), YPM VP 006263 (as *Tomistoma gavialoides*)
Eosuchus lerichei†: IRSNB 1740, IRSNB R 49
Eosuchus minor†: USNM 321933, USNM 181577, USNM 299730, USNM 418486
Euthecodon arambourgi†: MNHN ZEL 001
Eutretauranosuchus delfsi†: AMNH FR 570
Gavialis gangeticus: LDUCZ X1206, NHMUK 1935.6.4.1, NHMUK 2005.1601
Gavialis hysudricus†: NHMUK PV OR39805, NHMUK PV OR39808
Gavialis lewisi†: YPM VP 003226
Gavialosuchus eggenburgensis†: NHMUK PV R797 (cast)
Goniopholis felix†: YPM VP 000517
Goniopholis simus†: NHMUK PV OR41098
Gracilineustes leedsi†: NHMUK PV R2042, NHMUK PV R3014, NHMUK PV R3015, NHMUK PV R4762 (as *Metriorhynchus laeve*)
Hylaeochampsa vectiana†: NHMUK PV R177
Hyposaurus natator oweni†: YPM VP 000985
Kentisuchus spenceri†: NHMUK PV OR37717
Leidyosuchus canadiensis†: YPM VP 000284, NHMUK PV R10904 (cast)
Leidyosuchus gilmorei†: AMNH FR 5352

Listrognathosuchus multidentatis†: AMNH FR 5179 (as *Leidyosuchus multidentatis*)

Maroccosuchus zennaroi†: IRSNB R408

Mecistops cataphractus: NHMUK 1900.2.27.1, NHMUK 1904.9.9.2, NHMUK 1900.2.27.1, NHMUK 1862.6.30.8

Melanosuchus niger: NHMUK 1872.6.4.1, NHMUK unnumbered specimen, NHMUK 45.8.25.125

Nannosuchus gracilidens†: NHMUK PV OR48301, NHMUK PV OR48217

Navajosuchus novomexicanus†: AMNH FR 5186

Notosuchus terrestris†: NHMUK PV R14105

Osteolaemus tetraspis: LDUCZ X122, NHMUK 1862.6.30.5, NHMUK 1983.1130, NHMUK 1862.6.30.6

Paleosuchus trigonatus: NHMUK 1868.10.8.1

Pelagosaurus typus†: NHMUK PV R14437, NHMUK PV R19375, NHMUK PV R32598, NHMUK PV R32599, NHMUK PV R32600, NHMUK PV R32601, NHMUK PV R32602, NHMUK PV R36841

Pholidosaurus purbeckensis†: NHMUK PV R3414, NHMUK PV OR28432

Piscogavialis jugaliperforatus†: SMNK 1282 PAL

Planocrania datangensis†: IVPP V 5016

Planocrania hengdongensis†: IVPP V 6074

Prodiplocynodon langi†: AMNH FR 108

Protosuchus richardsoni†: AMNH FR 3024, AMNH FR 3025, AMNH FR 3026, AMNH FR 3027, AMNH FR 3028

Rhabdognathus keiniensis†: MNHN TGE 4031, MNHN TGE 3917, MNHN TGE 4360, MNHN TGE 4366

Rhabdognathus sp.†: MNHN TGE 4033

Rhamphosuchus crassidens†: NHMUK PV OR5265, NHMUK PV OR39802

Sarcosuchus imperator†: MNHN unnumbered complete skeleton in main exhibition

Sebecus icaeorhinus†: AMNH FR 3159, AMNH FR 3160, AMNH FR 3162

Shamosuchus djadochtaensis†: AMNH FR 6412

Steneosaurus bollensis†: SMNS complete unnumbered skeleton, SMNS 15391

Sunosuchus junggarensis†: IVPP V10606

Sunosuchus miaoi†: IVPP V500

Susisuchus anatoceps†: SMNK 3804 PAL

Terminonaris browni†: AMNH FR 5851 (as *Teleorhinus browni*)

Thecachampsa americana†: AMNH FR 5662, AMNH FR 5663 (as *Gavialosuchus americanus*), USNM 24939 (as *Tomistoma americana*)

Thecachampsa antiqua†: USNM 24938 (as *Gavialosuchus americanus*)

Theriosuchus pusillus†: NHMUK PV OR48330

Thoracosaurus macrorhynchus†: MNHN 1902–22, NHMUK PV R2798, NHMUK PV OR28296a, NHMUK PV OR28296b

Thoracosaurus neocesariensis†: NHMUK PV OR 41842 (cast)

Tomistoma cairense†: SMNS 10575, SMNS 50742, SMNS 50739, SMNS 50379a, SMNS 50734

Tomistoma dowsoni†: NHMUK PV R4769

Tomistoma petrolica†: IVPP V2303, IVPP V5015, IVPP unnumbered full skull

Tomistoma schlegelii: LDUCZ X1227, NHMUK 1848.10.31.19, NHMUK 1860.11.6.8, NHMUK no number, in wooden box

Vectisuchus leptognathus†: SMNS 50984

Voay robustus†: AMNH FR 3100, AMNH FR 3101, AMNH FR 3102, AMNH FR 3103, AMNH FR 3104, AMNH FR 3105, NHMUK PV R2026